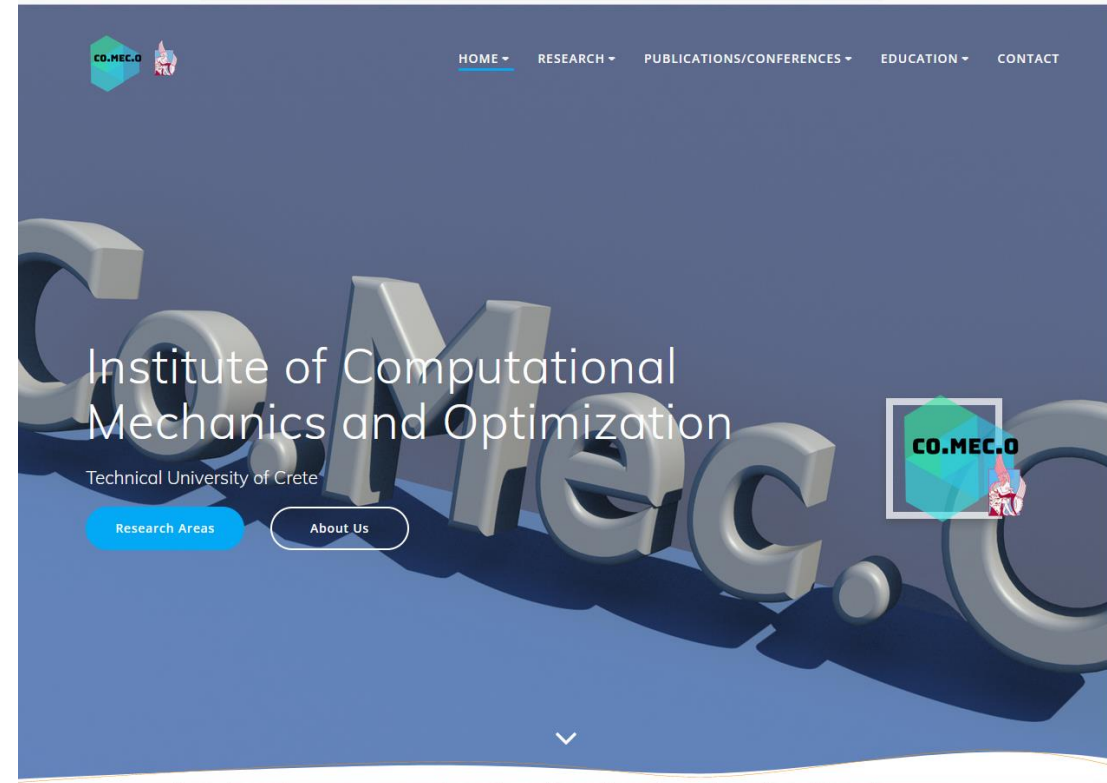


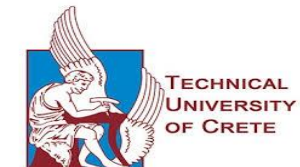
Microstructures, homogenization analysis and design

Prof. Georgios E. Stavroulakis

gestavroulakis@tuc.gr



www.comeco.tuc.gr



Microstructures

Lead to homogenized mechanical properties (orthotropic etc)

Can be tailored (graded materials, better than classical composites, suitable for AM)

In dynamics: band gap properties

Lead to mechanical metamaterials

Open questions: defects during construction, a lot of investigation related to 'missing ribs' etc

Technology limitations

Microstructures

In statics: homogenization

In dynamics: band gap properties (homogenization much more difficult, future work)

Homogenization

- Step 1
 - Study of a Representative sample in the microscopic scale (RVE)
 - Averaging (effective) material properties

- Step 2
 - Importing results in the macroscopic scale
 - Solution of the equivalent homogeneous structure

Mathematical framework of homogenization

- Starting with Hill-Mandel energy principle:

$$\boldsymbol{\sigma}^M : \boldsymbol{\epsilon}^M = \frac{1}{V_m} \int_{V_m} \boldsymbol{\sigma}^m : \boldsymbol{\epsilon}^m dV_m$$

- 3 loading states in the RVE boundaries satisfy this principle:
 - Linear displacements
 - Prescribed tractions
 - Periodic boundary conditions
- Linear displacements are chosen:

$$\mathbf{u}|_{\partial V_m} = \boldsymbol{\epsilon}^M \mathbf{x}$$

Mathematical framework of homogenization

- Calculation of the effective quantities:

$$\langle \boldsymbol{\epsilon} \rangle_{V_m} = \frac{1}{V_m} \int_{V_m} \boldsymbol{\epsilon}^m dV_m, \quad \langle \boldsymbol{\sigma} \rangle_{V_m} = \frac{1}{V_m} \int_{V_m} \boldsymbol{\sigma}^m dV_m$$

- Further simplification of the procedure

- For a perfectly bonded material:

$$\langle \boldsymbol{\epsilon} \rangle_{V_m} = \boldsymbol{\epsilon}^M$$

- Formulation for the average stresses:

$$\langle \boldsymbol{\sigma} \rangle_{V_m} = \frac{1}{V_m} \mathbf{f}\mathbf{x} = \boldsymbol{\sigma}^M$$

Mathematical framework of homogenization

- Estimation of the effective elasticity tensor:

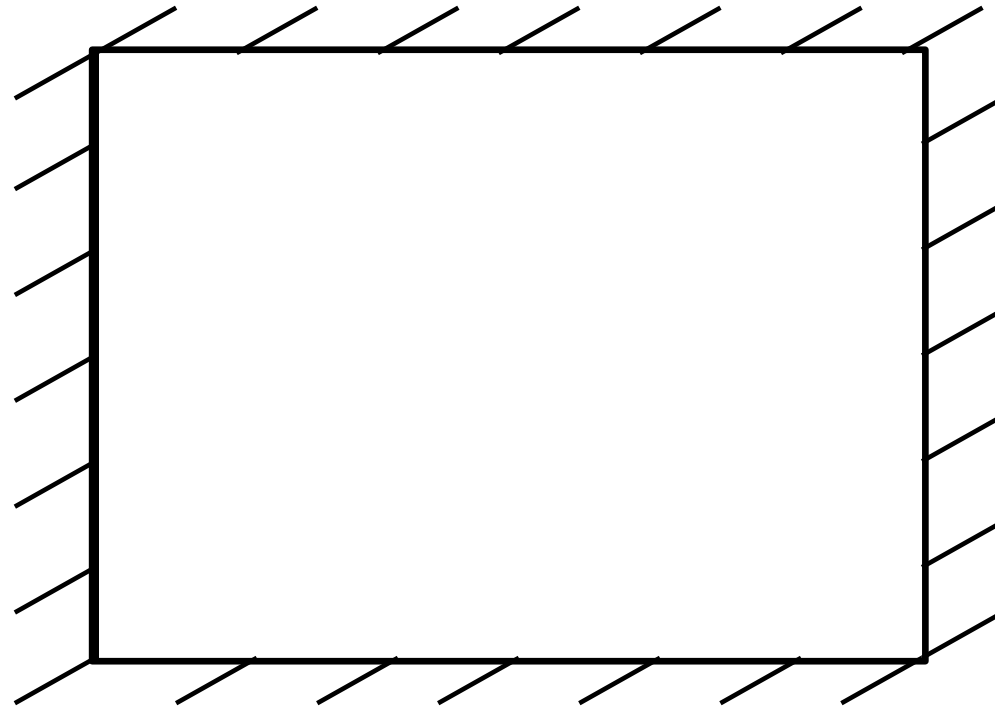
$$\langle \boldsymbol{\sigma} \rangle_{V_m} = \mathbf{E}^* \langle \boldsymbol{\epsilon} \rangle_{V_m}$$

- Effective elasticity tensor: 9 unknowns
- Thus, 3 loadings of the RVE=>9 equations

Zohdi T.I., Wriggers P. (2008), *An Introduction to Computational Micromechanics*, Springer, The Netherlands.

Example 2

Classical homogenization scheme

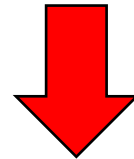


Loading: Linear displacement boundary conditions

Example 2: Results

For material characteristics:

- A. Strong material (existing): $E=1$, $\nu=0.3$
- B. Soft material (non-existing): $E=0.007$, $\nu=0.007$



Effective properties:

E_{xx}	E_{yy}	ν_{xy}	ν_{yx}	G_{xy}
0.066	0.067	-0.2433	-0.2484	0.0117

- Good comparison with topology optimization: Effective Poisson ratio = -0.192

Simpler analytical homogenization: star-shaped and derivatives

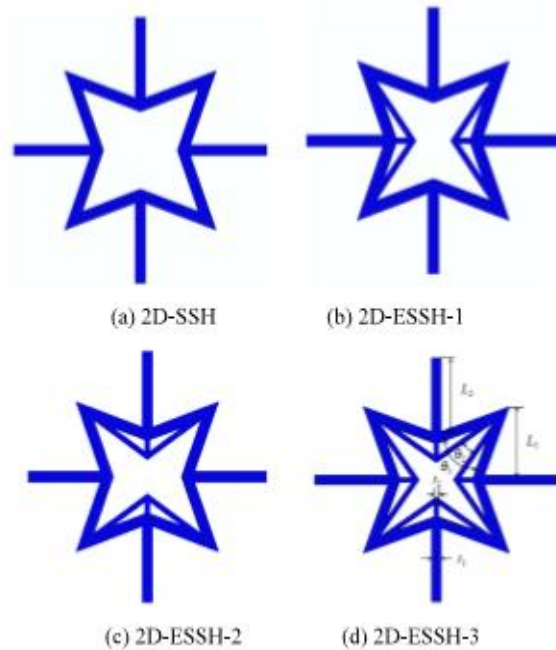
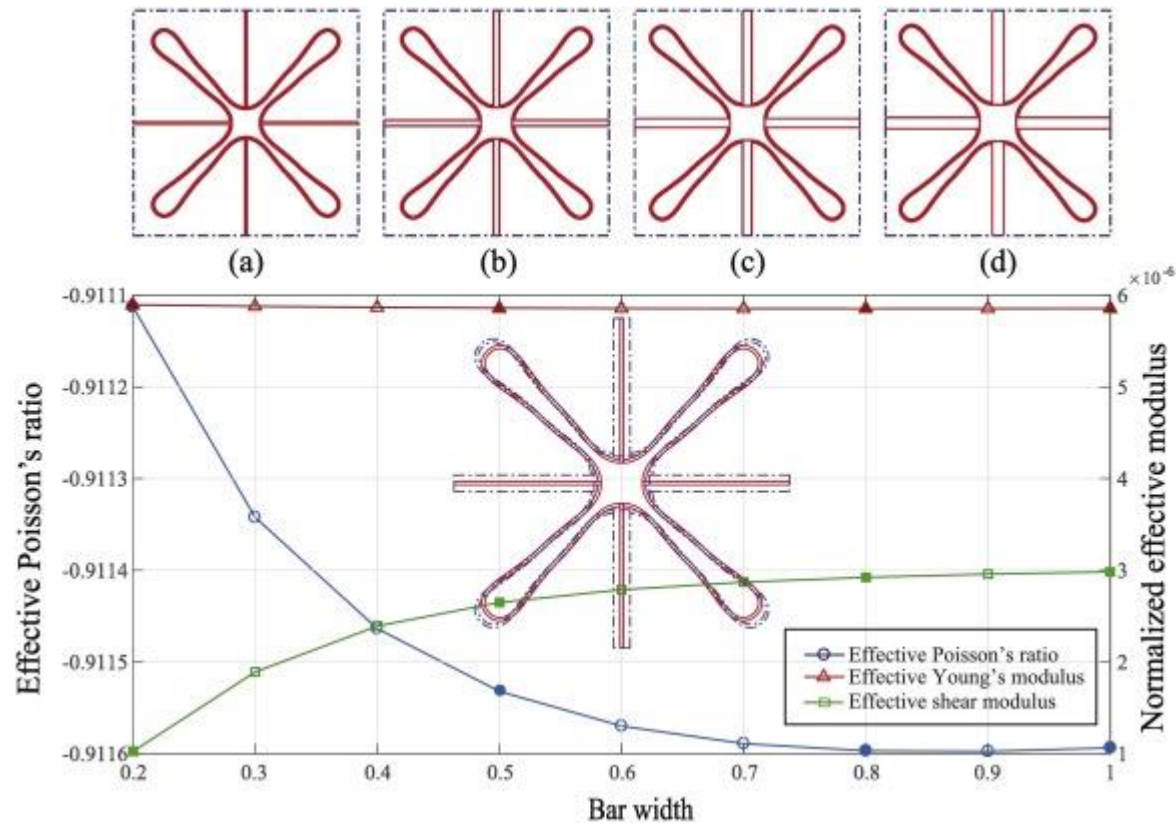


Fig. 1. Four kinds of structures.

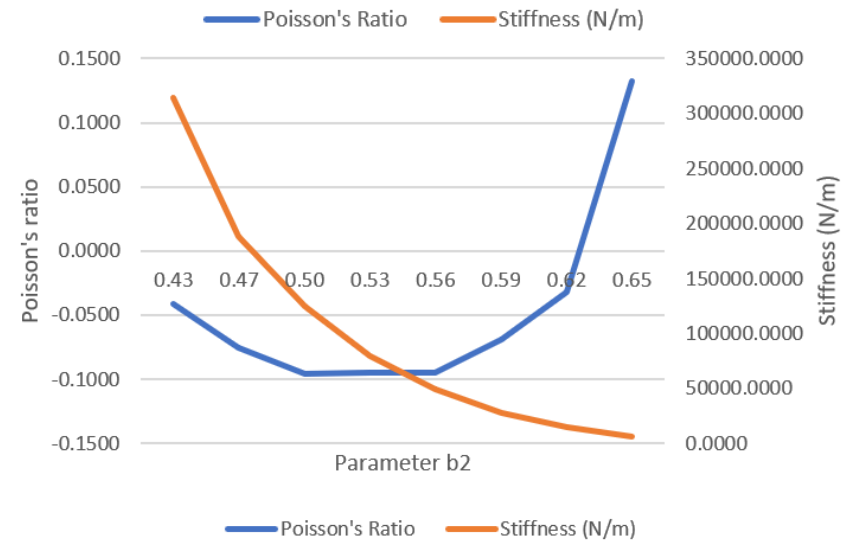
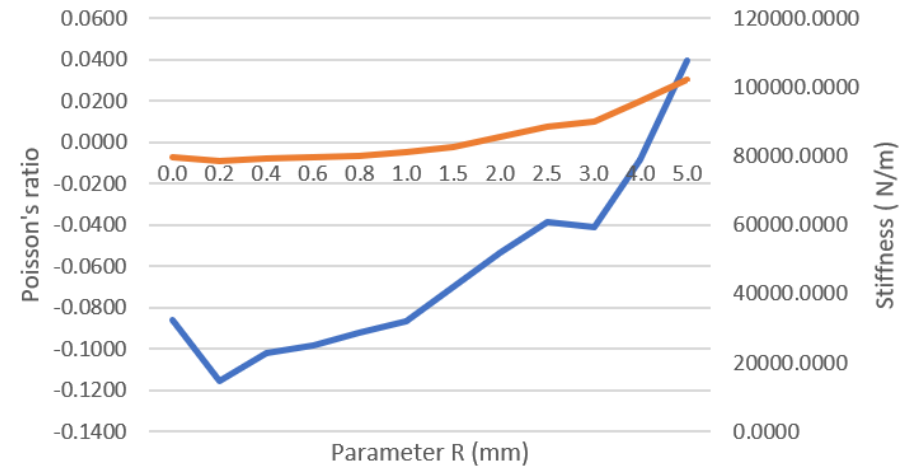
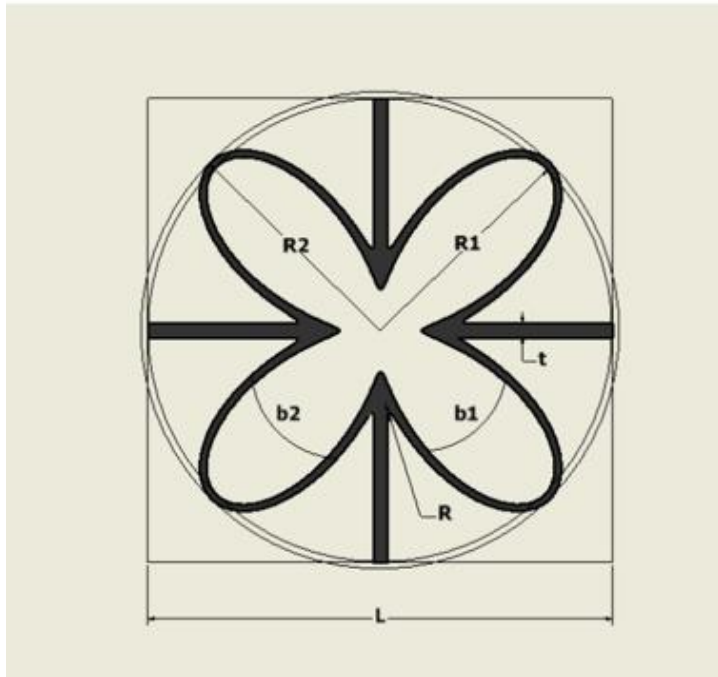
Na Xu, Hai-Tao Liu, Ming-Ran An, Liang Wang,
Novel 2D star-shaped honeycombs with enhanced effective
Young's modulus and negative Poisson's ratio,
Extreme Mechanics Letters, Volume 43, 2021, 101164, ISSN
2352-4316, <https://doi.org/10.1016/j.eml.2020.101164>.

Simpler analytical homogenization: petal auxetics



Deepak Kumar Pokkalla, Zhen-Pei Wang, Leong Hien Poh, Ser Tong Quek, Isogeometric shape optimization of smoothed petal auxetics with prescribed nonlinear deformation, *Computer Methods in Applied Mechanics and Engineering*, Volume 356, 2019, Pages 16-43, ISSN 0045-7825, <https://doi.org/10.1016/j.cma.2019.07.014>.

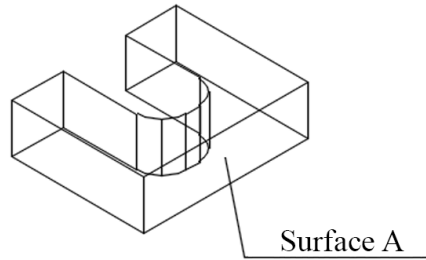
Cookie-shaped auxetics



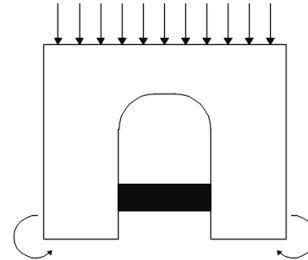
Koustoumpardis, C.-G. and Stavroulakis, G. (2023) "Mechanical properties of cookie-shaped auxetics using finite elements and soft robotics application", *Technische Mechanik - European Journal of Engineering Mechanics*, 43(2), pp. 230–237. doi: 10.24352/UB.OVGU-2023-059.

Cookie-shaped auxetics

a)

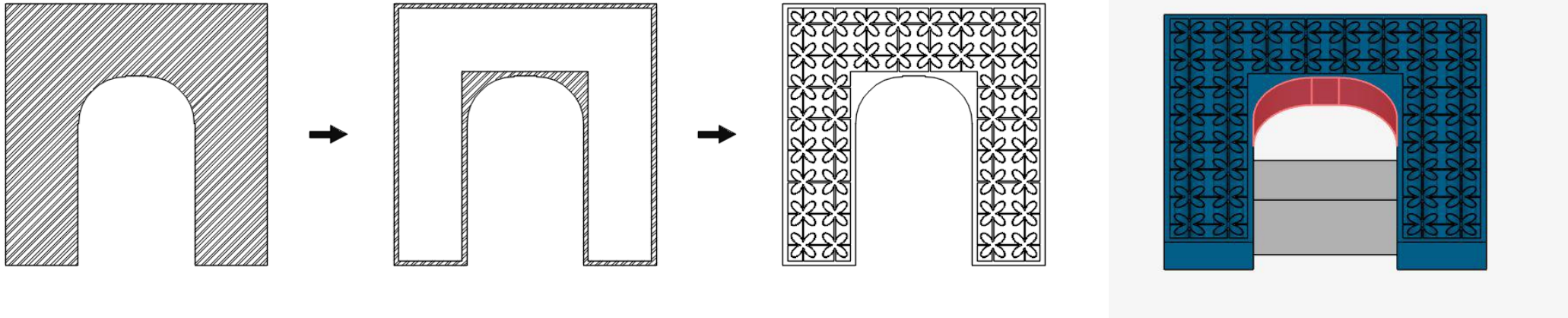


b)



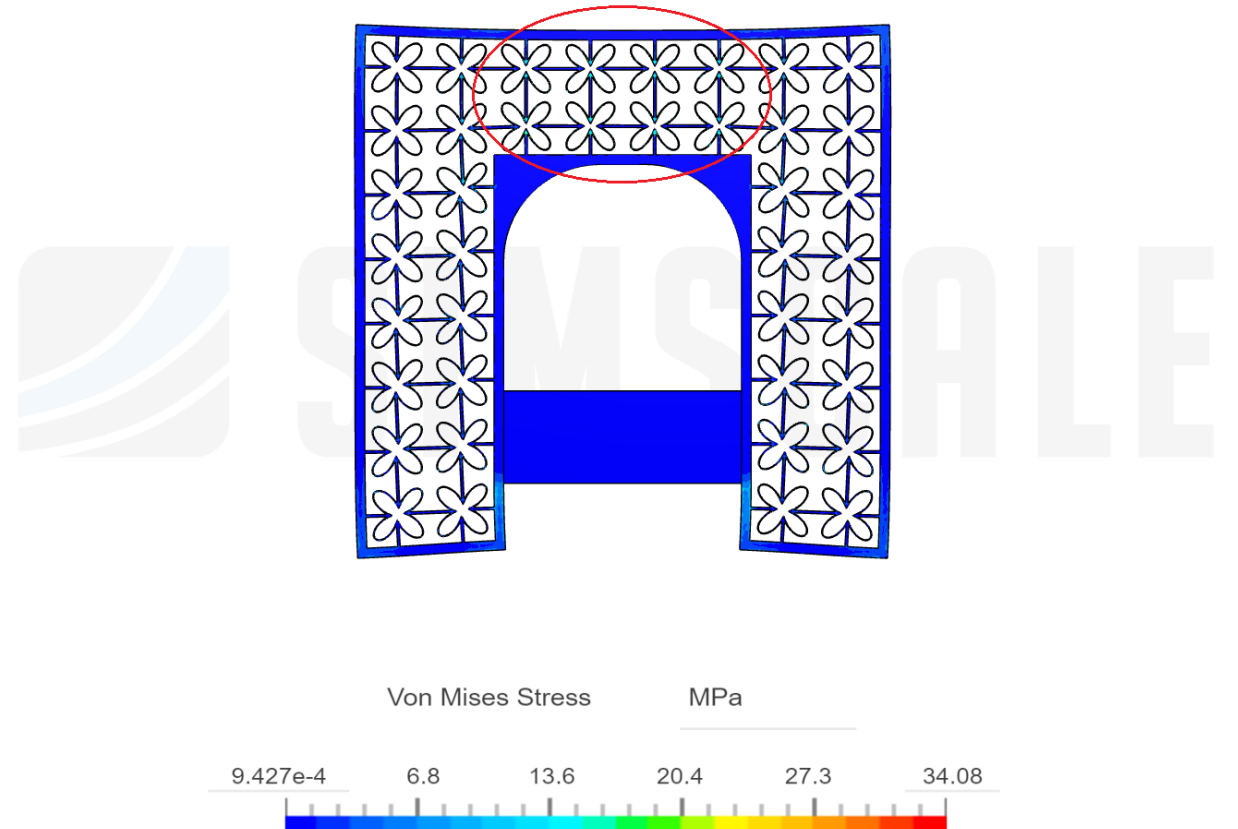
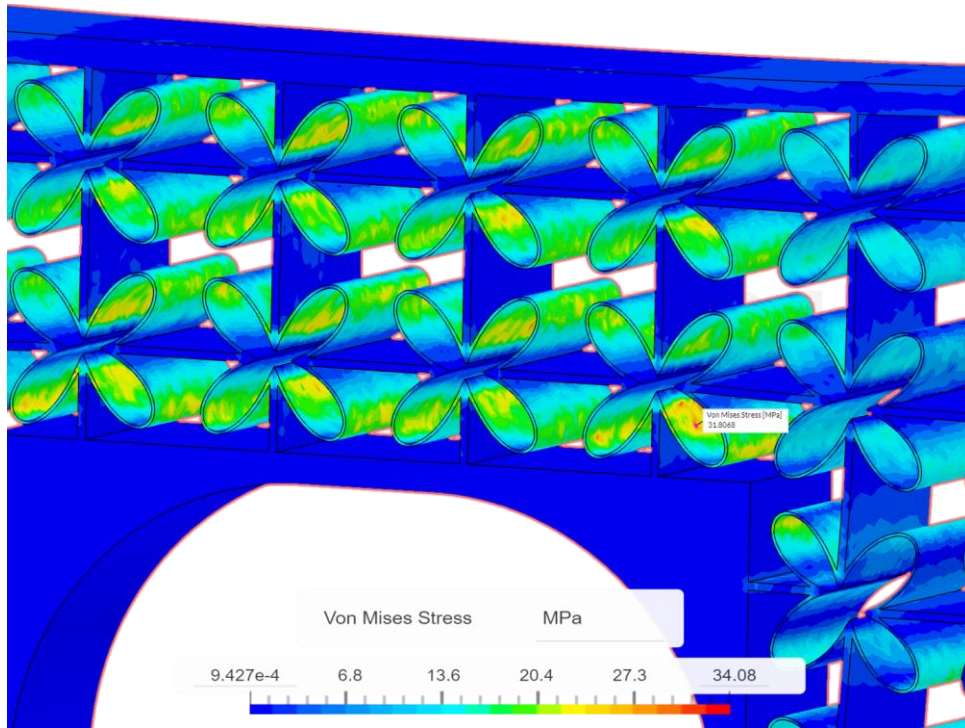
Koustoumpardis, C.-G. and Stavroulakis, G. (2023)
“Mechanical properties of cookie-shaped auxetics using finite elements and soft robotics application”, *Technische Mechanik - European Journal of Engineering Mechanics*, 43(2), pp. 230–237. doi: 10.24352/UB.OVGU-2023-059.

Cookie-shaped auxetics



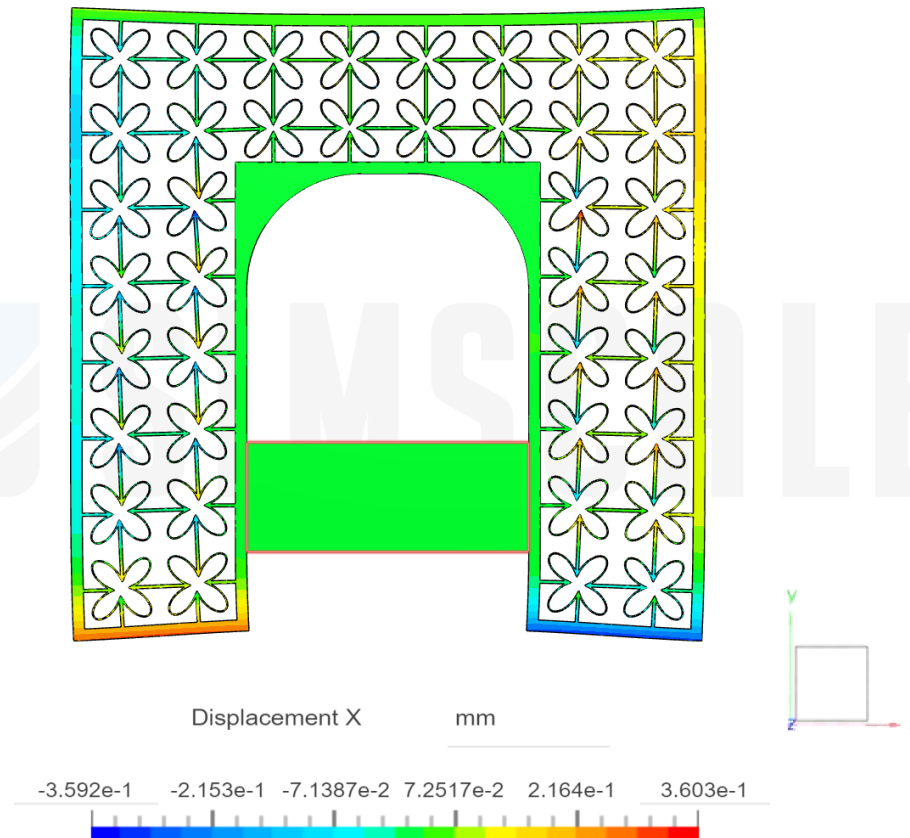
Koustoumpardis, C.-G. and Stavroulakis, G. (2023)
“Mechanical properties of cookie-shaped auxetics using finite elements and soft robotics application”, *Technische Mechanik - European Journal of Engineering Mechanics*, 43(2), pp. 230–237. doi: 10.24352/UB.OVGU-2023-059.

Cookie-shaped auxetics



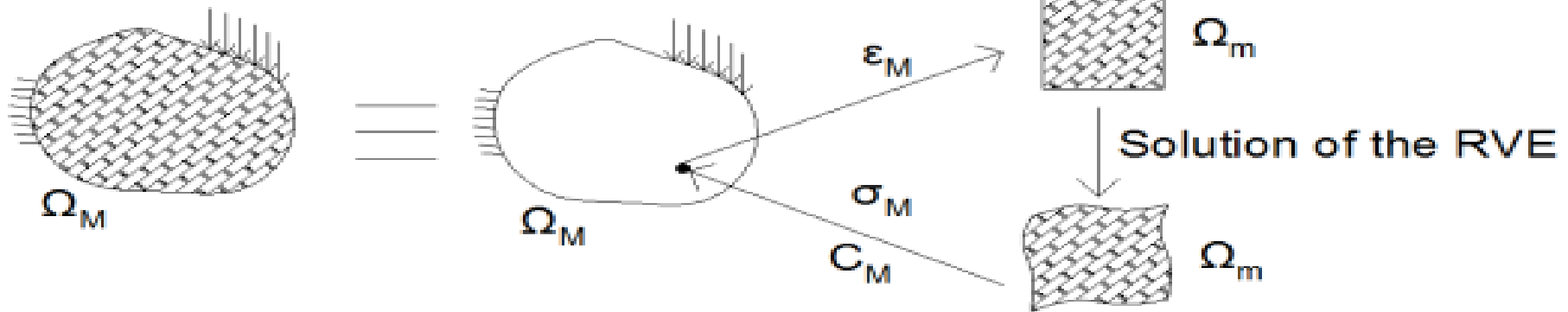
Koustoumpardis, C.-G. and Stavroulakis, G. (2023)
“Mechanical properties of cookie-shaped auxetics using finite elements and soft robotics application”, *Technische Mechanik - European Journal of Engineering Mechanics*, 43(2), pp. 230–237. doi: 10.24352/UB.OVGU-2023-059.

Cookie-shaped auxetics



Koustoumpardis, C.-G. and Stavroulakis, G. (2023)
“Mechanical properties of cookie-shaped auxetics using finite elements and soft robotics application”, *Technische Mechanik - European Journal of Engineering Mechanics*, 43(2), pp. 230–237. doi: 10.24352/UB.OVGU-2023-059.

Data-driven homogenization + usage

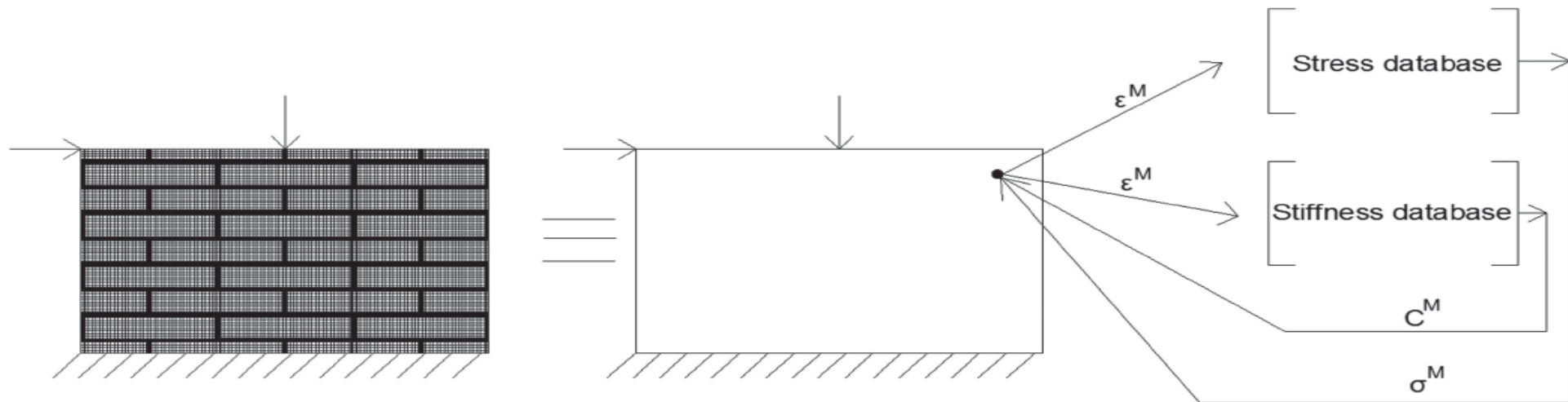


Classical fe^2 multi-scale homogenization

Each RVE represents the non-linear behaviour of the heterogeneous structure

Data-driven schemes

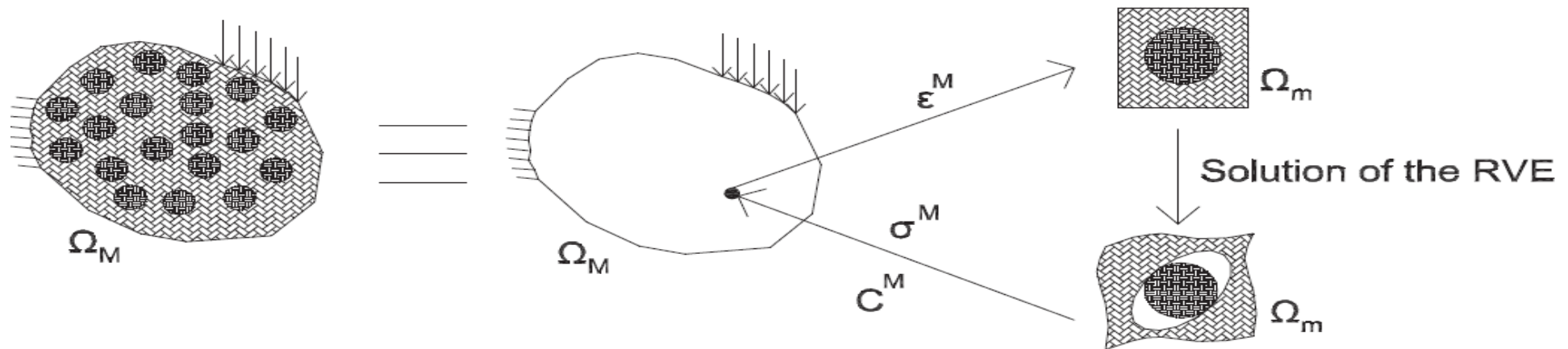
- A. Database interpolation providing the constitutive stress-strain response
- B. Usage of machine learning tools Most often: **Artificial Neural Networks (ANN)** Training, using data sets



G. Drosopoulos, K. Giannis, M. Stavroulaki, G. Stavroulakis, *Metamodeling-Assisted Numerical Homogenization for Masonry and Cracked Structures*, CE, J. Eng. Mech, 2018

Computational homogenization

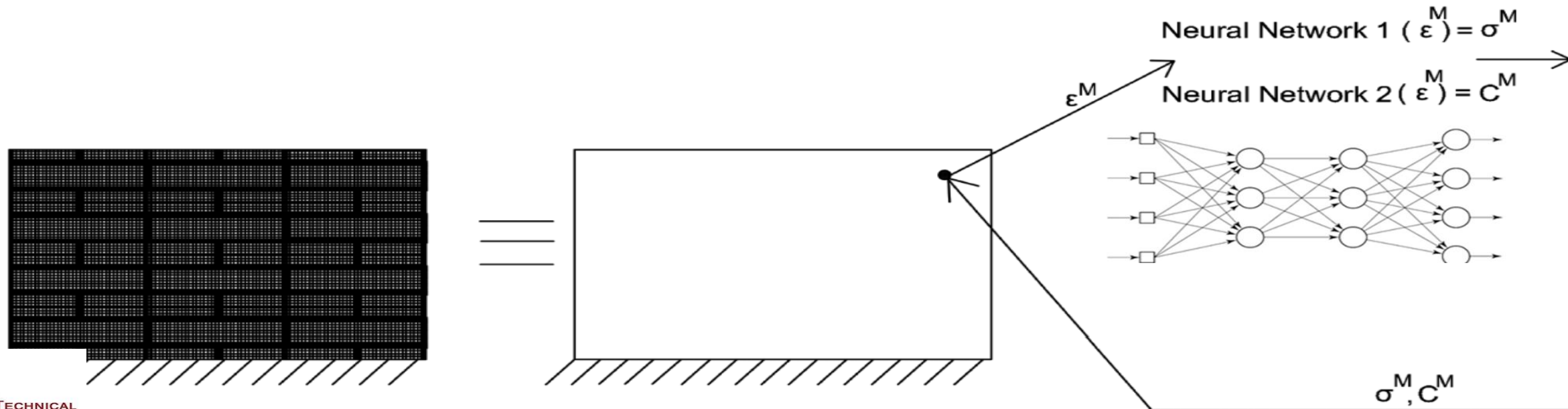
- Conventional **FE²**
- Solve a Representative Volume Element (RVE)
- For every Gauss point of the macro structure
- Within increments-iterations of Newton-Raphson



G. Drosopoulos, P. Wriggers, G. Stavroulakis, *A multi-scale computational method including contact for the analysis of damage in composite materials*, *Comput. Mater. Sci.*, 2014

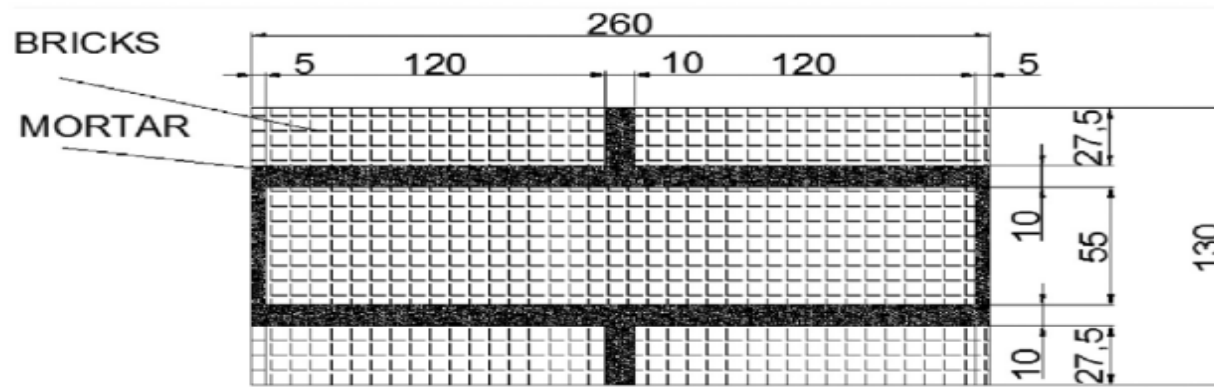
Data-driven computational homogenization

- Substitutes microscopic simulations by a trained ANN
- Providing the effective stress-strain response
- Training takes place “offline” -> increased efficiency



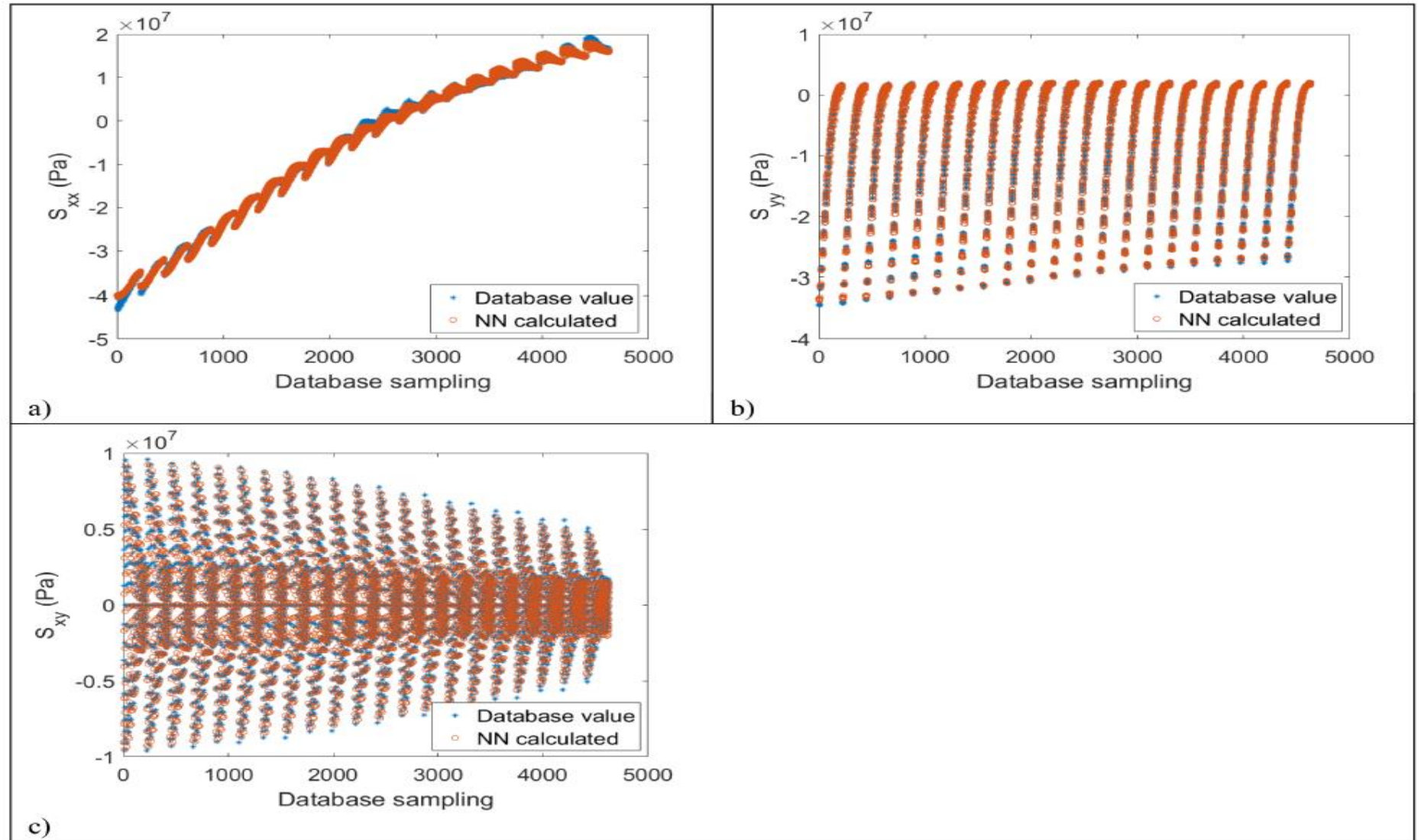
Applications to masonry structures

- Drucker-Prager material law is used for the mortar joints
- To depict damage of the RVE



	Young's modulus (GPa)	Poisson's ratio	Tensile strength (MPa)	Compressive strength (MPa)
Bricks	4,865	0,09	-	-
Mortar joints	1,180	0,06	0,9	3,2

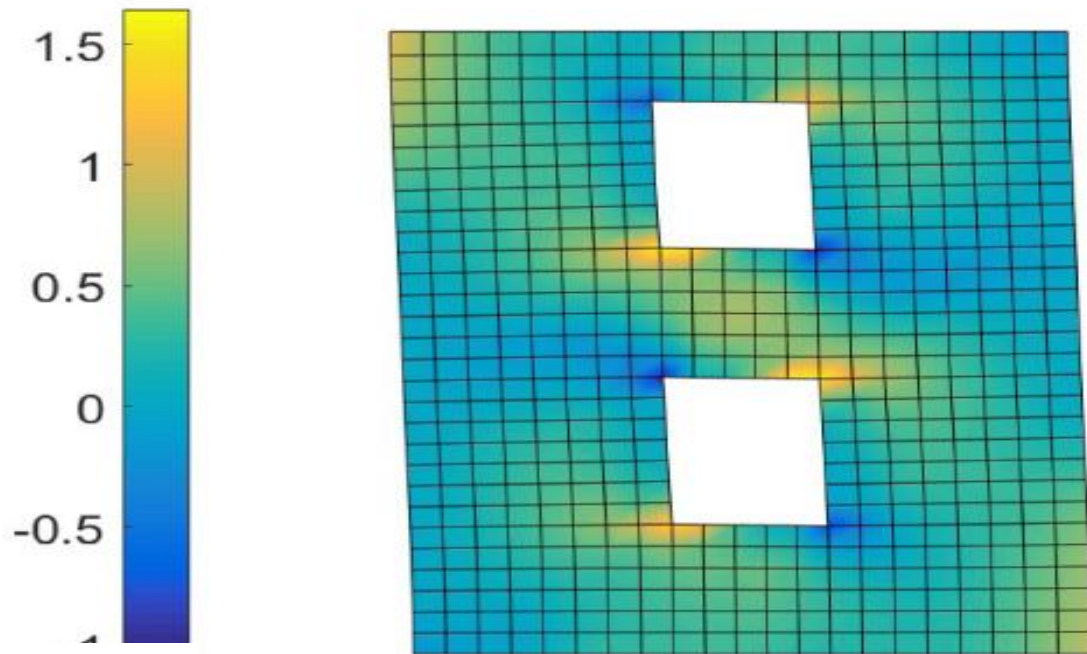
Verification of stress-strain training



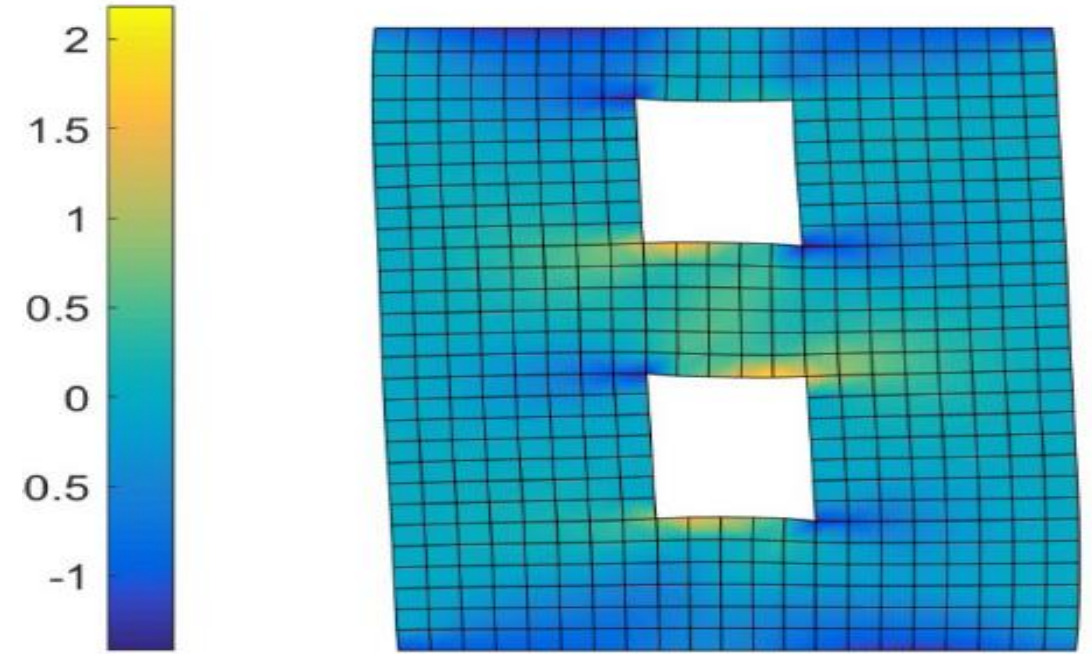
Masonry wall with openings

- Max principal stresses

Interpolation FE²



Proposed ANN- FE²

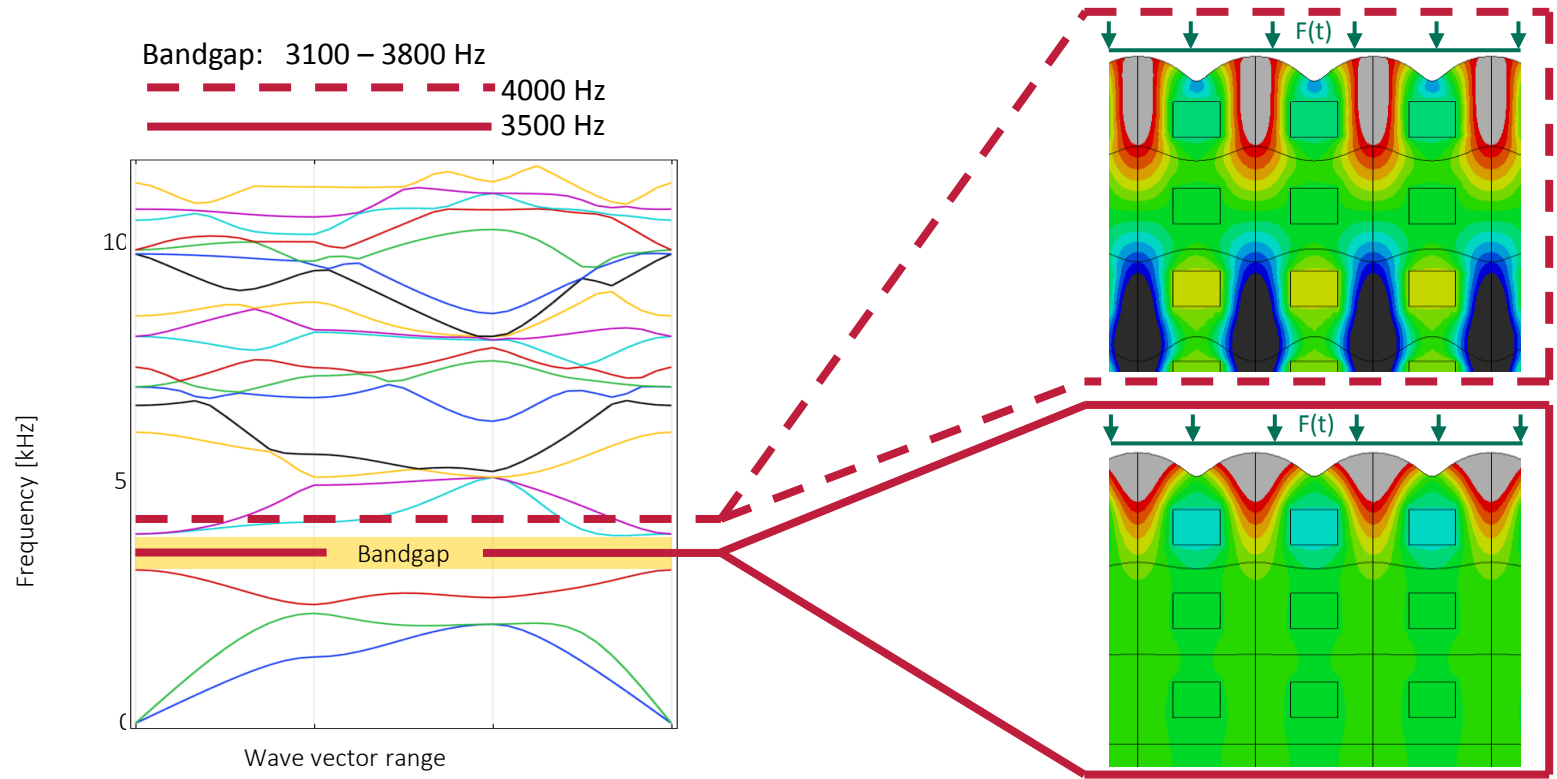
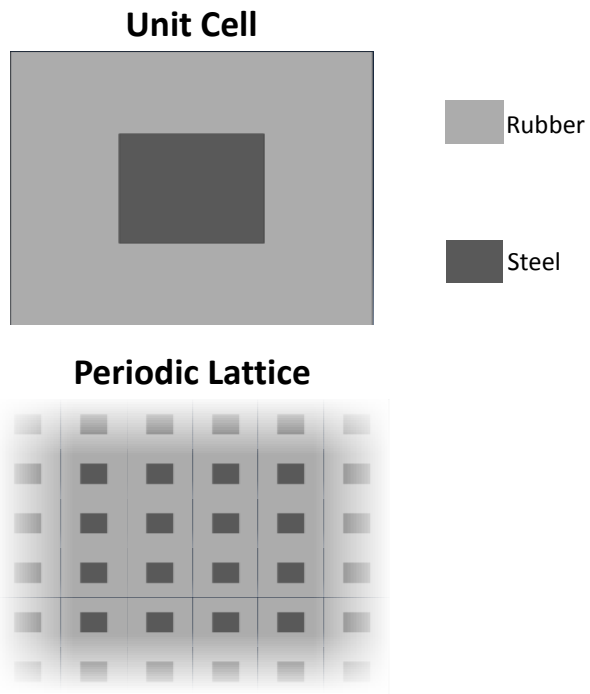
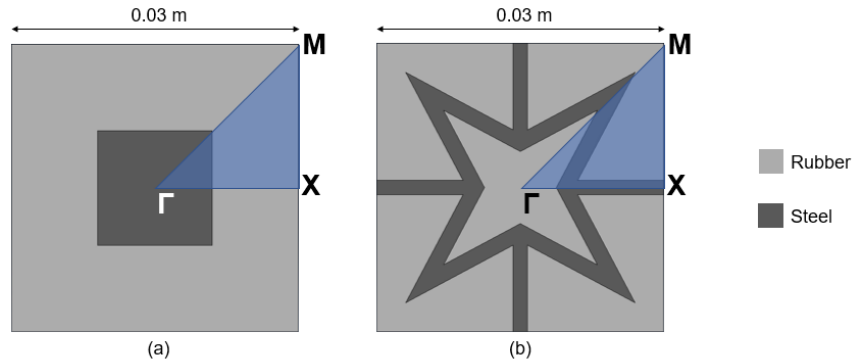


Microstructures

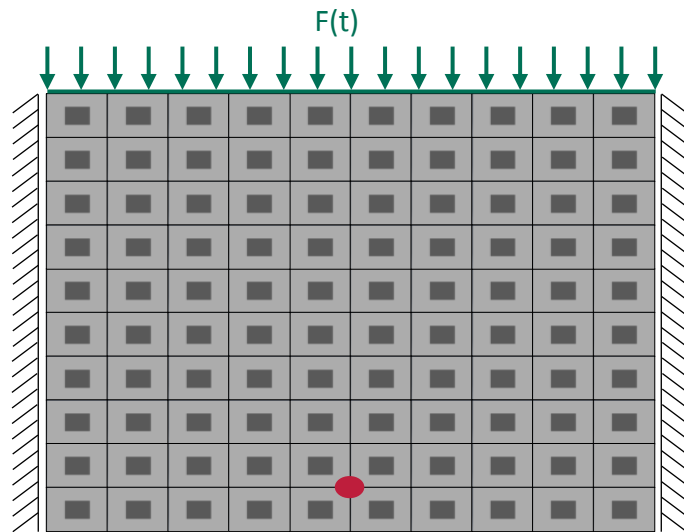
In statics: homogenization

In dynamics: band gap properties (homogenization much more difficult, future work)

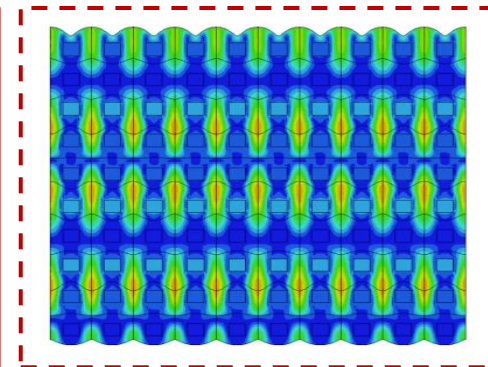
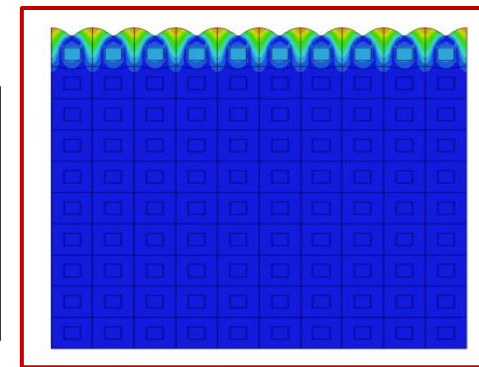
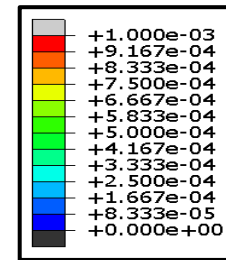
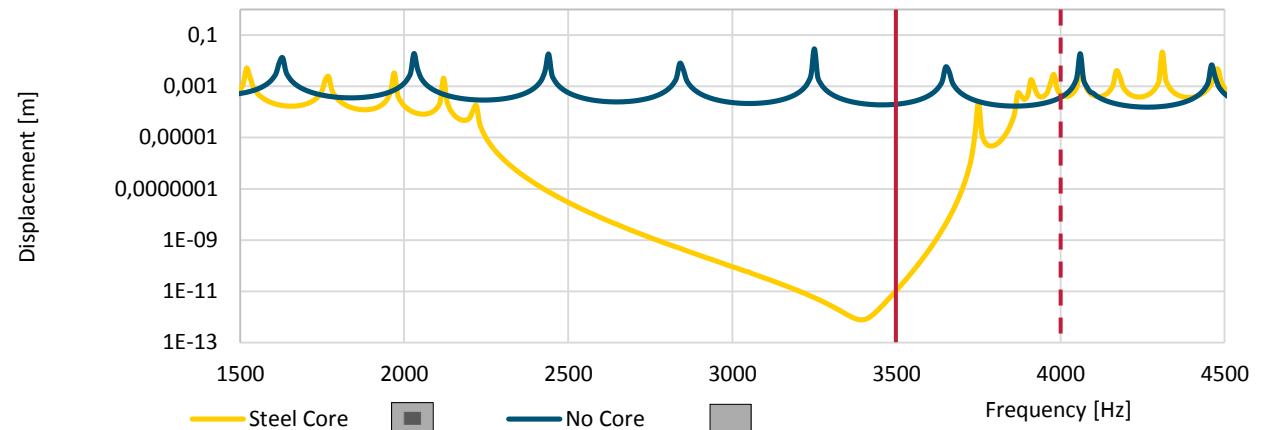
Resonant Unit Cell



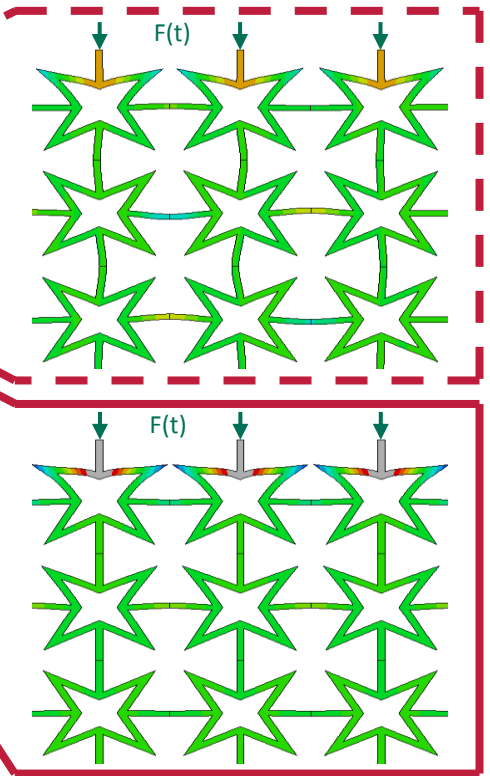
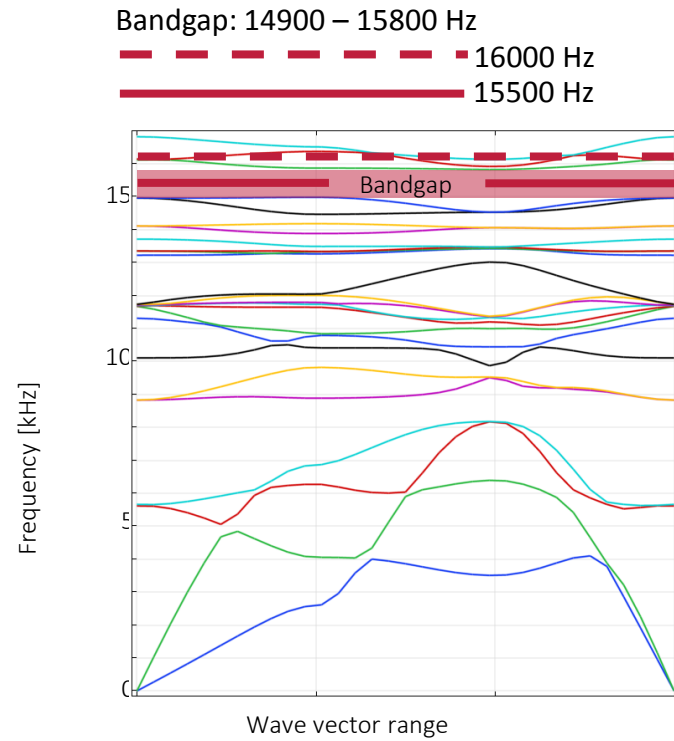
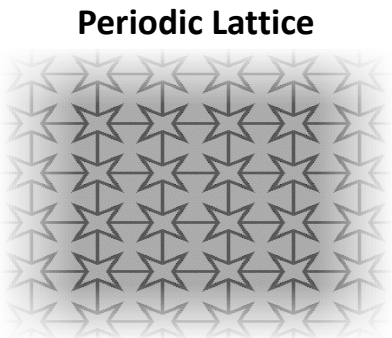
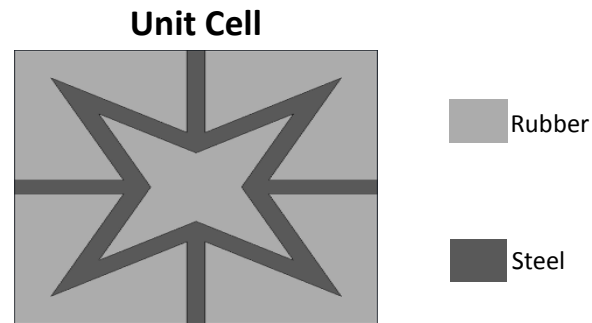
Resonant Lattice: Composite with band gaps



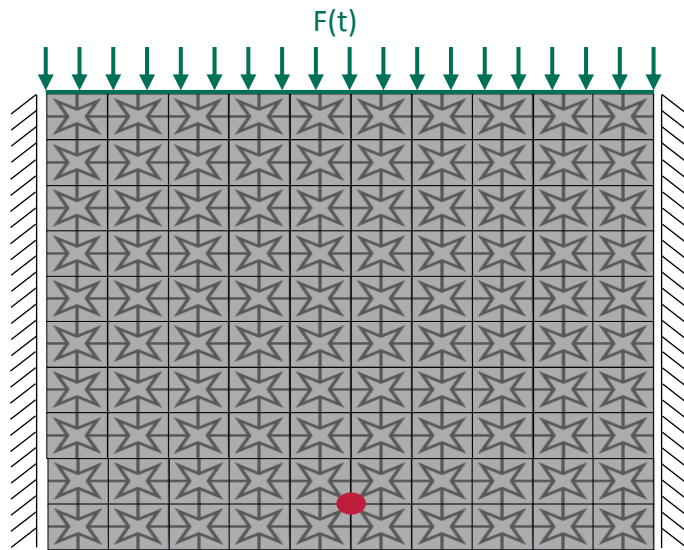
- 10 by 10 resonant unit cells
- Harmonic pressure load on top surface
- Oscillations measured at the bottom ()



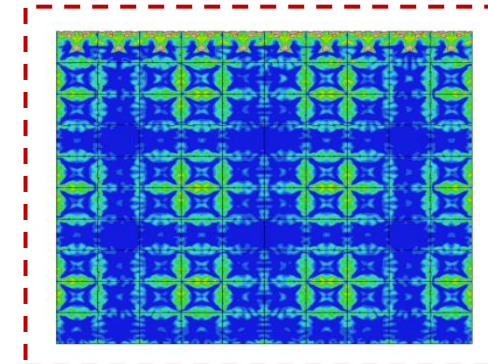
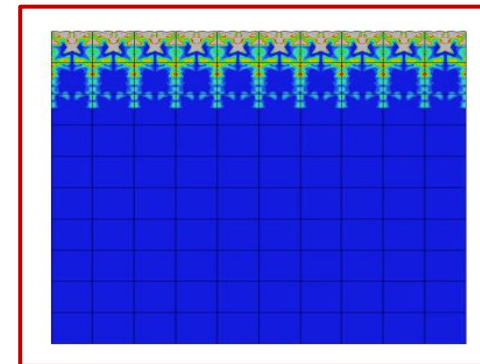
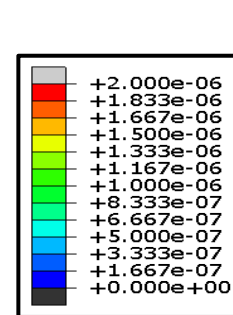
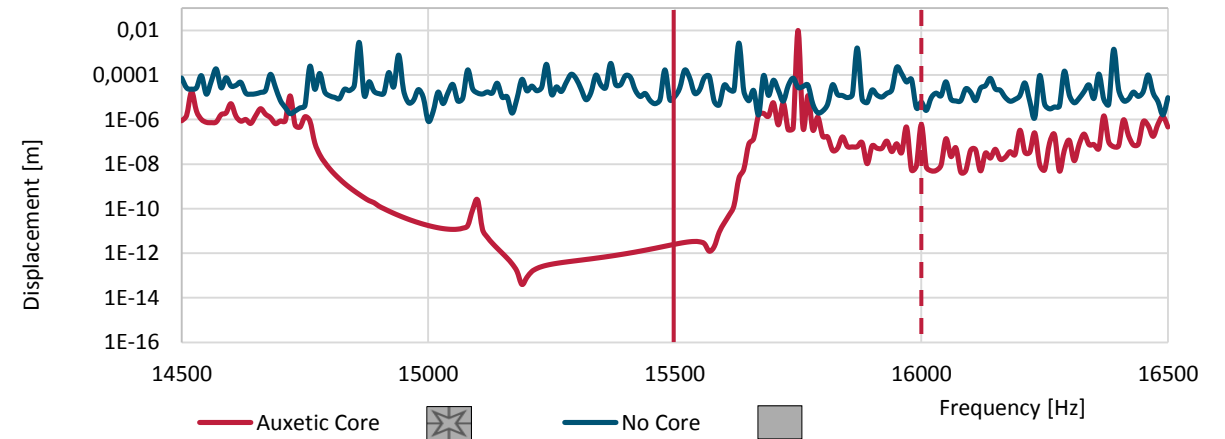
Auxetic Unit Cell: metamaterial with band gaps



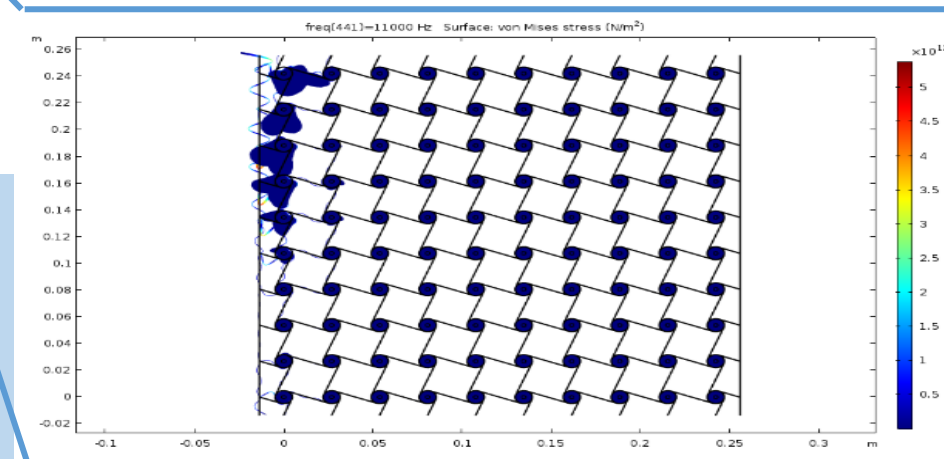
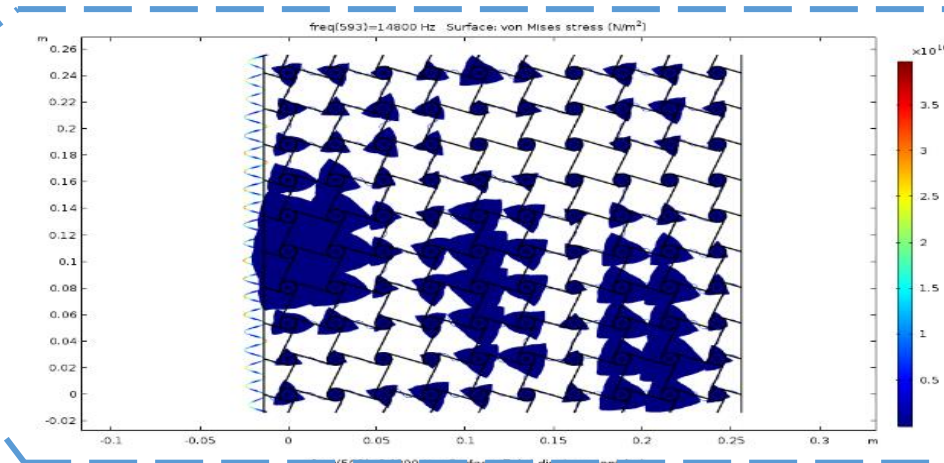
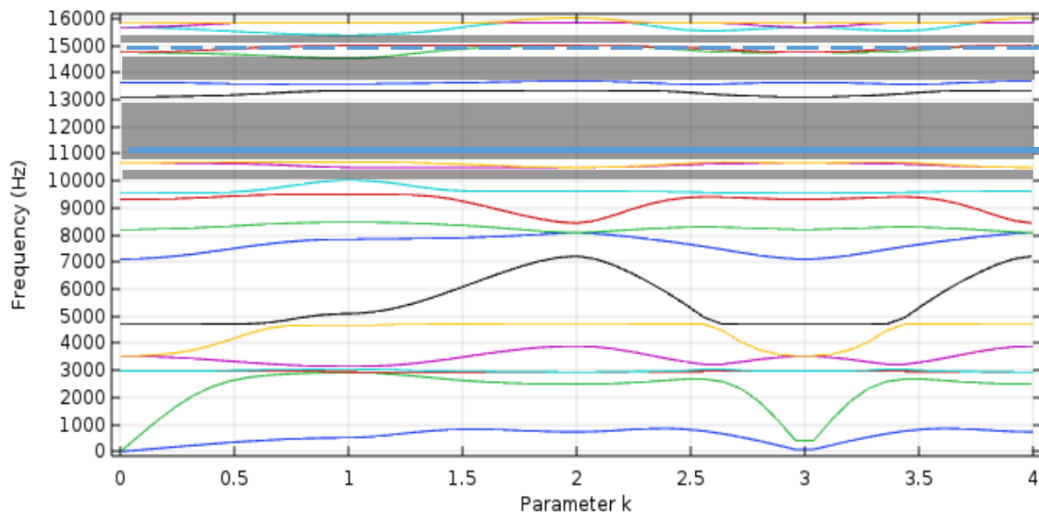
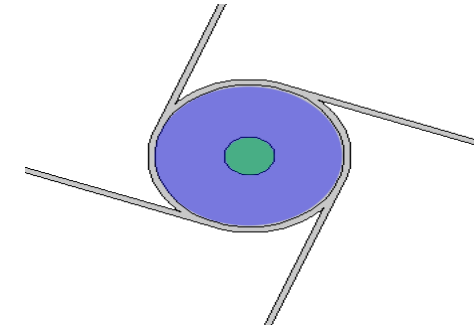
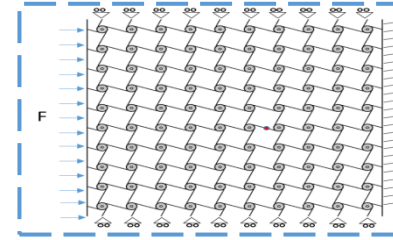
Auxetic Lattice and band-gap formation



- 10 by 10 auxetic unit cells
- Harmonic pressure load on top core surface
- Oscillations measured at the bottom ()



Chiral microstructures With band gaps



Chinis, D.; Stavroulakis, G.E. Band Gap Analysis for Materials with Cookie-Shaped Auxetic Microstructures, Using Finite Elements. *Appl. Sci.* **2023**, *13*, 2774. <https://doi.org/10.3390/app13052774>

Bloch theory

The whole lattice can be obtained from the correlation of the unit cell

The displacement $q(r_j)$ of the lattice points of the unit cell for the case of plane waves

$$q(r_j) = q_j e^{(i\omega t - kr_j)}$$

where

q_j is the amplitude

ω is frequency

k is the wave vector

Bloch theory

According to the Bloch's theorem, the displacement at the j^{th} point in any cell can be identified

$$q = q(r_j)e^{k(r-r_j)} = q(r_j)e^{(k_1n_1+k_2n_2)}$$

where:

$$k_1 = k e_1 = \delta_1 + i\varepsilon_1$$

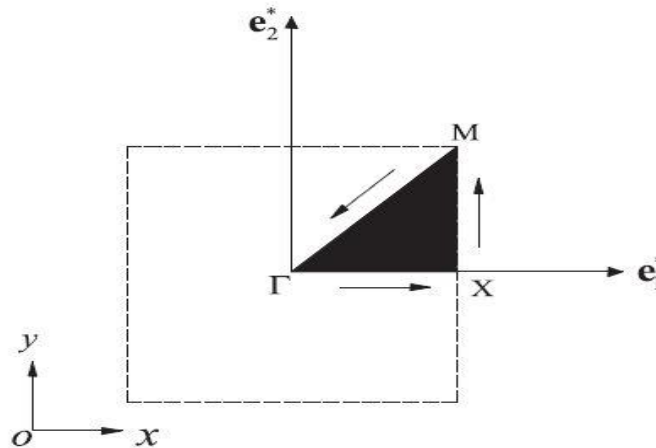
$$k_2 = k e_2 = \delta_2 + i\varepsilon_2$$

k_1 and k_2 denote the components of wave vector k which dissipates along the vectors e_1 and e_2

δ denotes the attenuation constant

Bloch theory

The possible extraction of band gaps is based on the assumption of wave vectors which are following the first Brillouin zone and the irreducible Brillouin zone (Γ -X-M)



In general, periodic structures are systems with identical segments, coupled to their neighboring. More specifically, uniform 2-D structures can be considered as a special case of periodic structures which are homogeneous in x and y

Bloch theory

Finite element model of a rectangular segment with a 4-noded rectangular element

$$q = [q_1^T \ q_2^T \ q_3^T \ q_4^T]$$

where

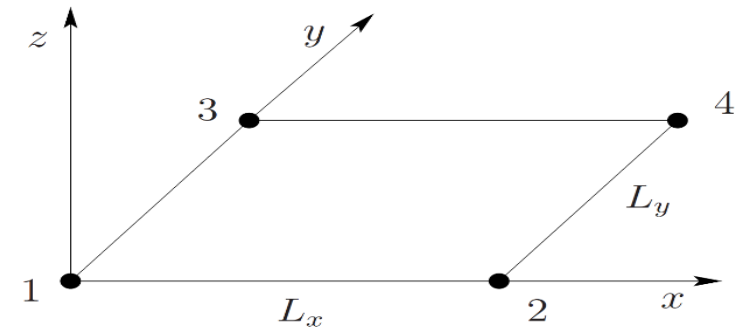
q_j are the nodal degrees of freedom of the nodes of the j th corner

The equation of motion of the element of reference is given as

$$(-\omega^2 M + i\omega C + K)q = f$$

where

M , C and K are the mass, damping and stiffness matrices respectively, ω is the natural frequency, f is the loading vector and i the imaginary number



Bloch theory

The propagation of the wave can then be obtained from the so-called propagation constants

$$\mu_x = \kappa_x L_x$$

$$\mu_y = \kappa_y L_y$$

which in turn, provide the relation among the periodic displacements q on the sides of the periodic element as:

$$q_2 = \lambda_x q_1$$

$$q_3 = \lambda_y q_1$$

$$q_4 = \lambda_x \lambda_y q_1$$

where: $\lambda_x = e^{-i\mu_x}$ $\lambda_y = e^{-i\mu_y}$

As a result, the nodal degrees of freedom can be rewritten as:

$$q = \Lambda_R q_1$$

where



$$\Lambda_R = [I \ \lambda_x I \ \lambda_y I \ \lambda_x \lambda_y I]$$

Bloch theory

In the free response case, a possible equilibrium at node 1 gives that nodal forces of every element which is connected to node 1 is zero. Thus, we have:

$$\Lambda_L f = 0$$

where:

$$\Lambda_L = \begin{bmatrix} I & \lambda_x^{-1} I & \lambda_y^{-1} I & (\lambda_x \lambda_y)^{-1} I \end{bmatrix}$$

The modal equations can be reformed as:

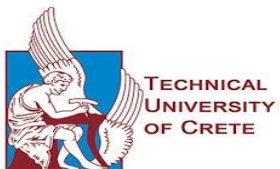
$$\left(-\omega^2 \bar{M}(\mu_x, \mu_y) + i\omega \bar{C}(\mu_x, \mu_y) + \bar{K}(\mu_x, \mu_y) \right) q = f$$

where $\bar{M} = \Lambda_L M \Lambda_R$, $\bar{K} = \Lambda_L K \Lambda_R$ and $\bar{C} = \Lambda_L C \Lambda_R$ are the reduced matrices.

The eigenvalue problem can be written as:

$$\bar{D}(\omega, \lambda_x, \lambda_y) = 0$$

where \bar{D} is the reduced dynamic stiffness matrix.



Optimization problem

Objective Function

Maximize the Band Gap Area

Constraints

Symmetry design constraints

e.g. at y axis: $n2 < 1$

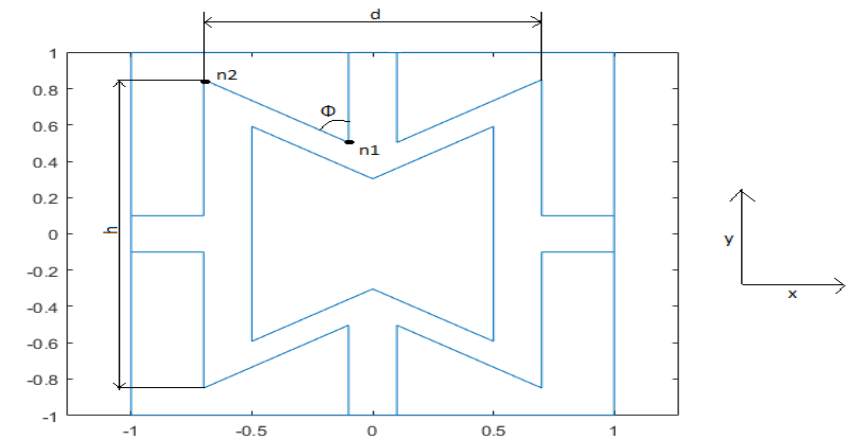
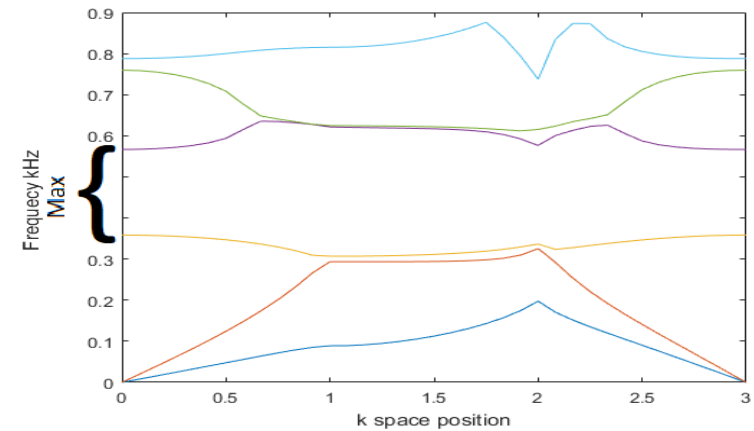
at x axis: $n1 < 0$, etc.

Design Variables:

Height: $h \in [0.2, 1.9]$

Width: $d \in [0.2, 1.9]$

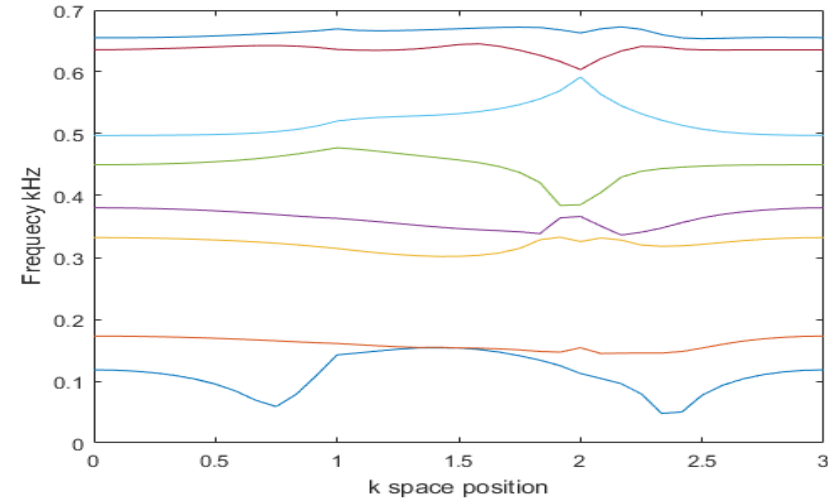
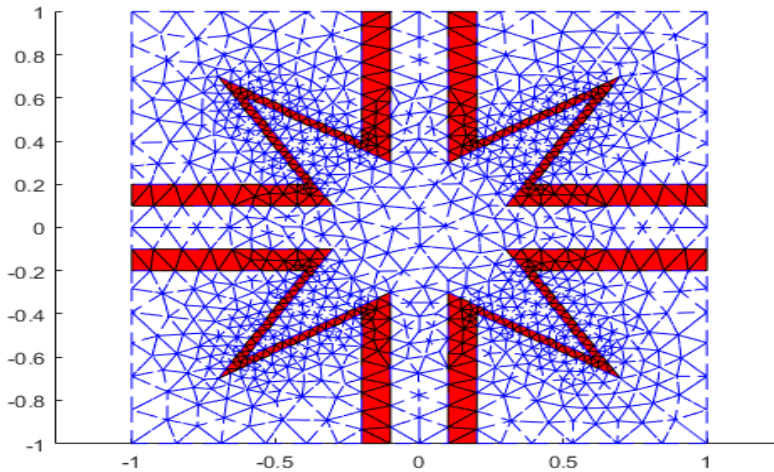
Angle: $\Phi \in [50^\circ, 120^\circ]$



Numerical results

Star-shaped unit cell

Star shape unit cell with 0.1m thickness



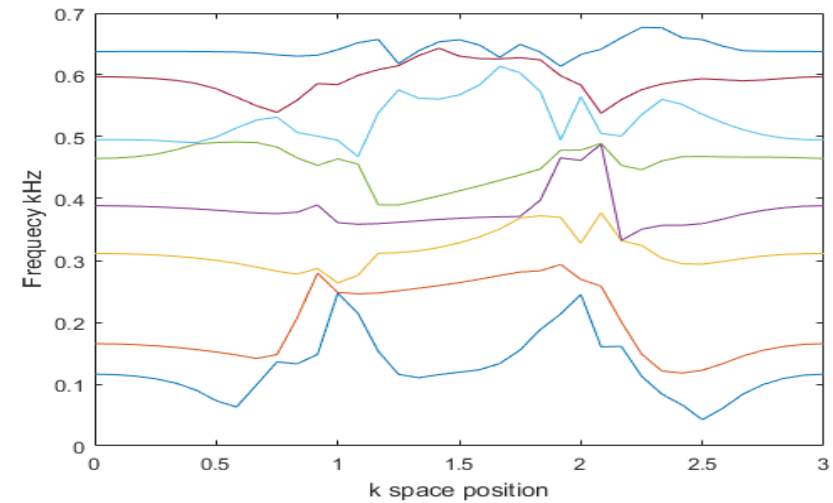
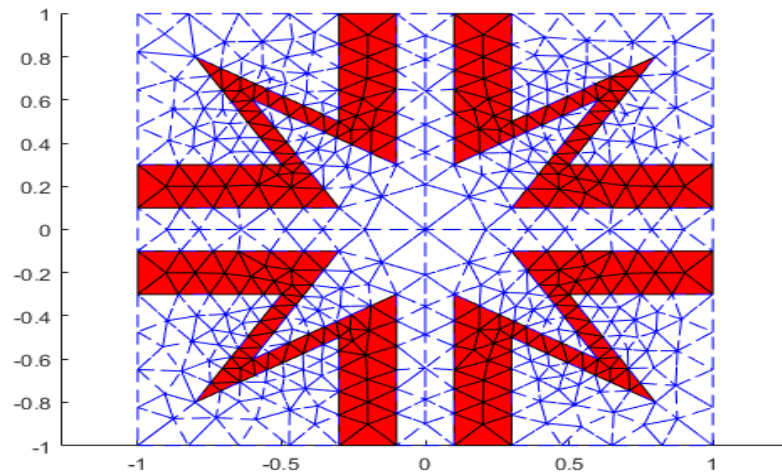
Square unit cell with auxetic core with thickness=0.1m and its dispersion curve

The band gaps appear in a lot of regions, like between second and third eigenvalues

Numerical results

Star-shaped unit cell

Star shape unit cell with 0.2m thickness



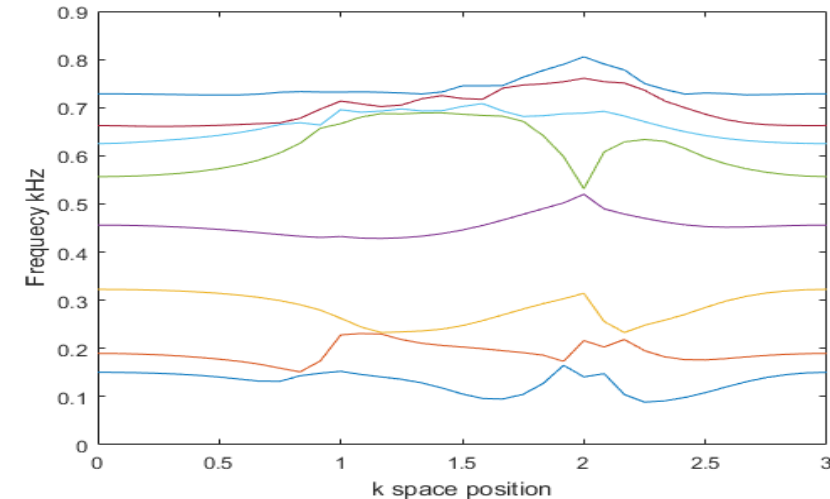
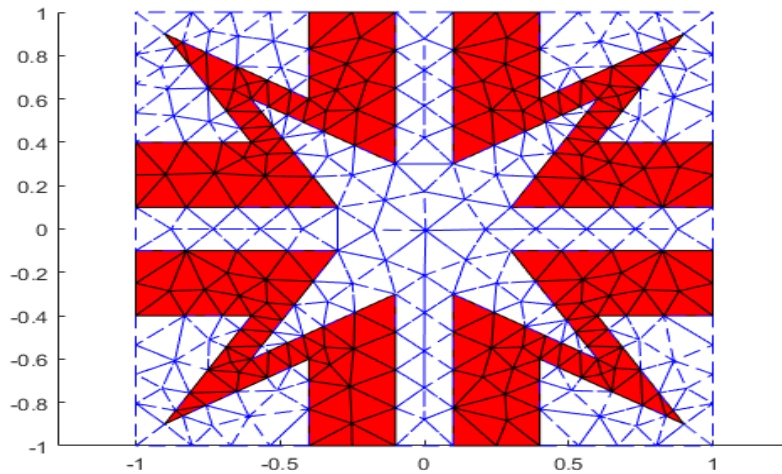
Square unit cell with auxetic core with thickness=0.2m and its dispersion curve

The band gaps do not appear in this case

Numerical results

Star-shaped unit cell

Star shape unit cell with 0.3m thickness



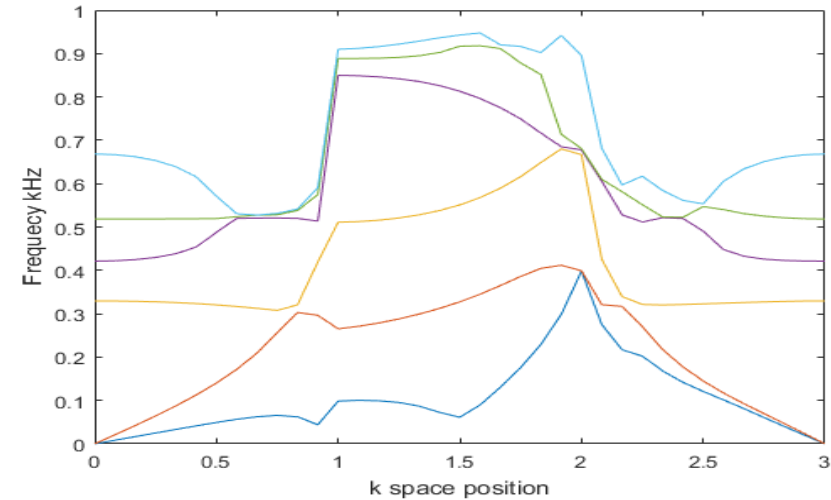
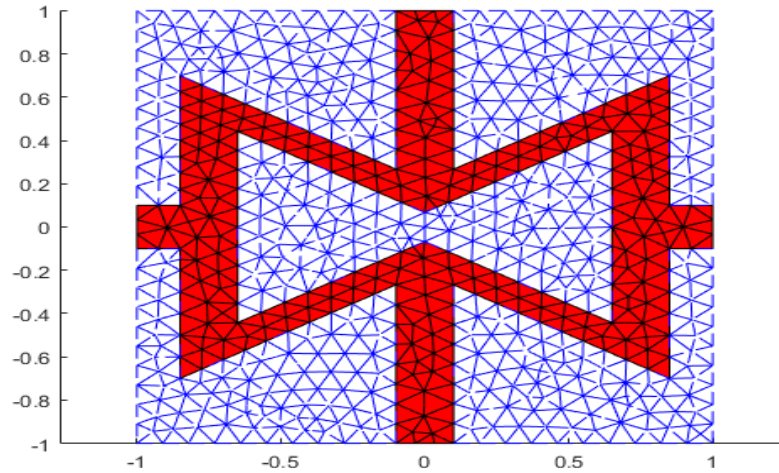
Square unit cell with auxetic core with thickness=0.3m and its dispersion curve

The band gaps appear in a lot of regions, however they are narrower compared to the case of thickness which equals to 0.1m.

Numerical results

Hexagon-shaped unit cell

$h=1.4m$, $d=1.7m$, $b=0.2m$, $\Phi=60^\circ$



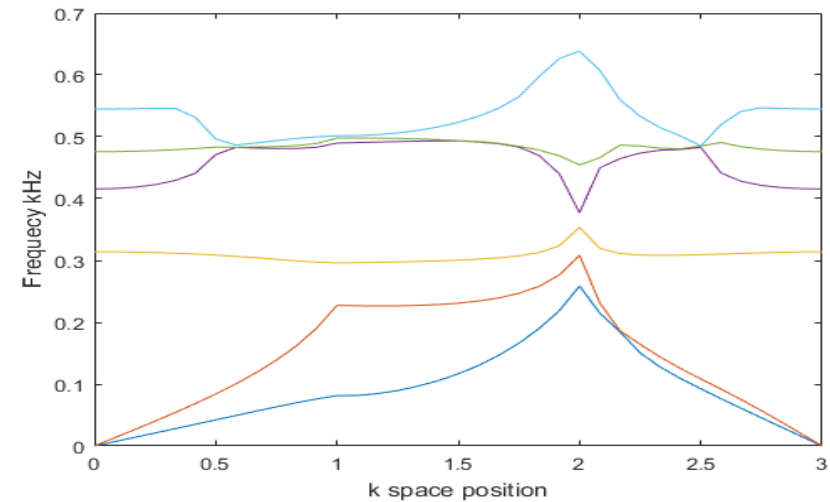
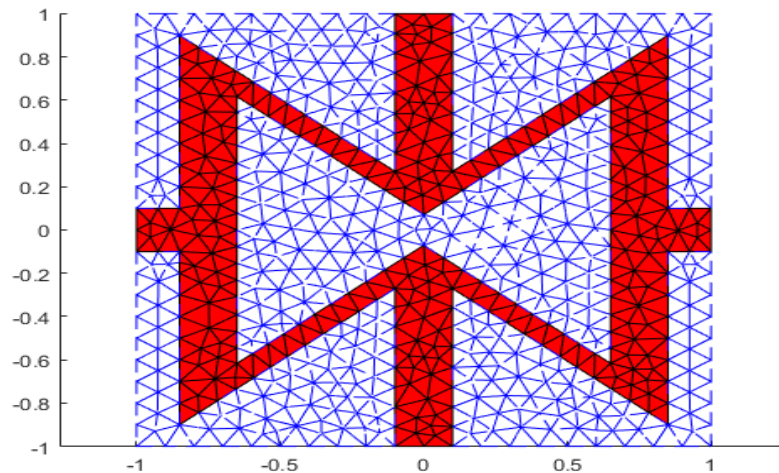
Square unit cell with hexagon auxetic core its dispersion curve

The band gaps do not appear in this case

Numerical results

Hexagon-shaped unit cell

$h=1.8\text{m}$, $d=1.7\text{m}$ $b=0.2\text{m}$, $\Phi=60^\circ$



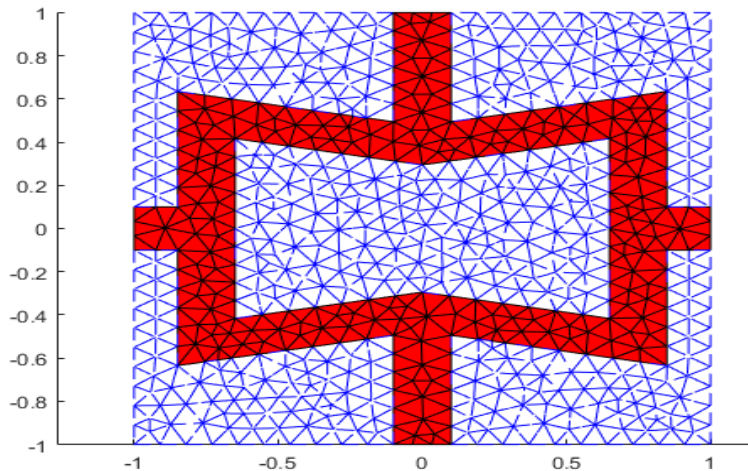
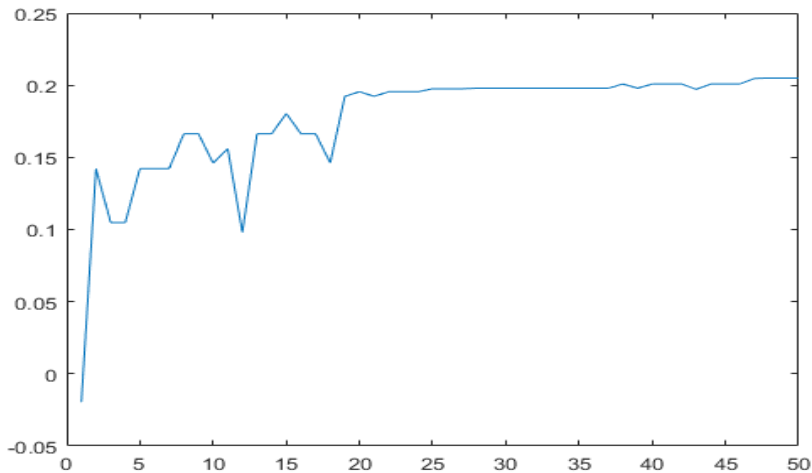
Square unit cell with hexagon auxetic core its dispersion curve

In the case band gaps appear between 3rd and 4th eigenvalues, and the frequency range is equal to 23.3Hz.

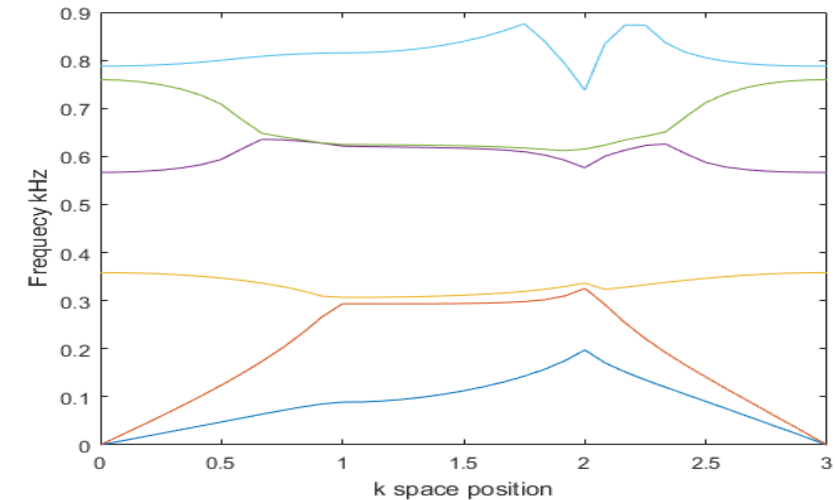
Numerical results

Optimized hexagon-shaped auxetic unit cell

Optimization the band gap between 3rd and 4th in order to achieve auxetic behavior.



Optimized core of the unit cell



The optimized values of the design variables are:
Angle $\Phi=78.4^\circ$, Height $h=1.27m$, Width $d=1.69m$
Maximum Range= 214Hz

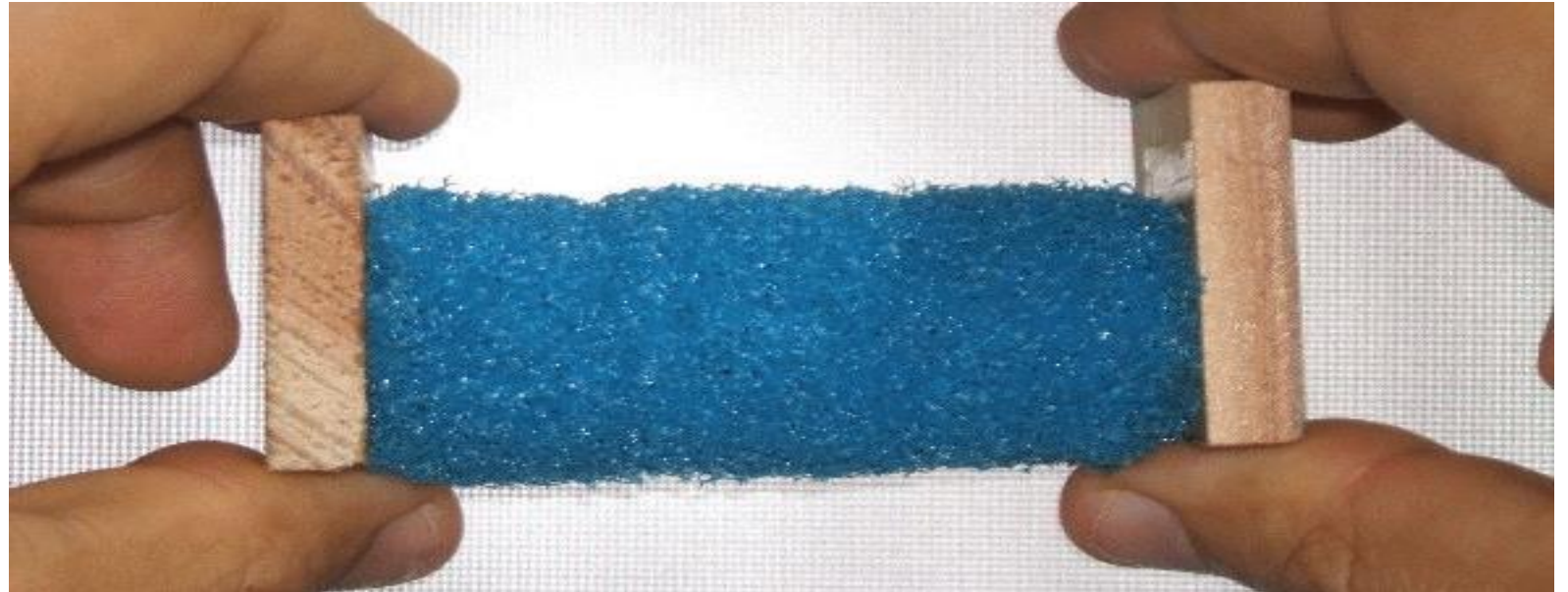
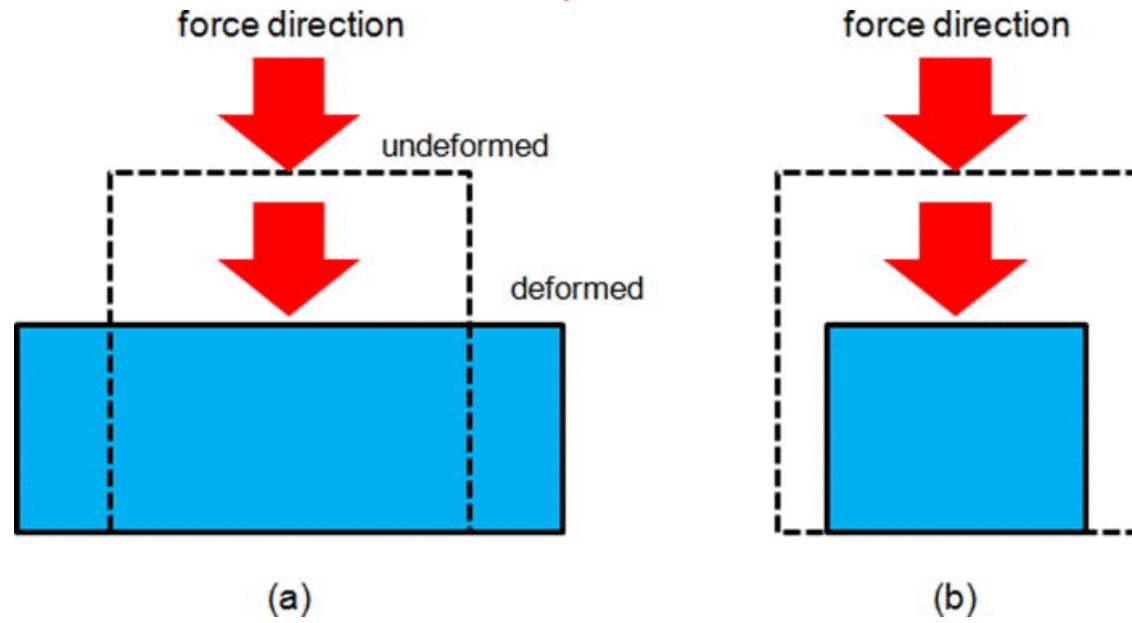
*Model example:
Auxetics and technological applications*

Negative Poisson's ratio

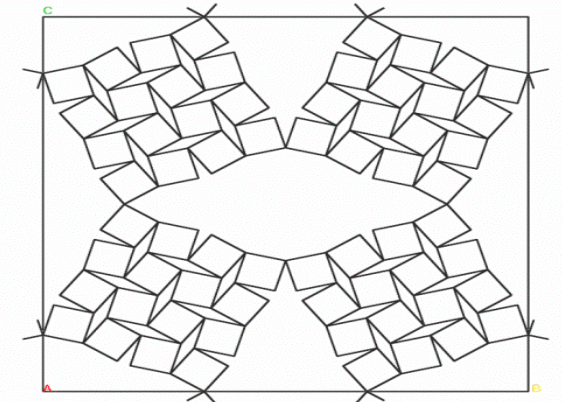
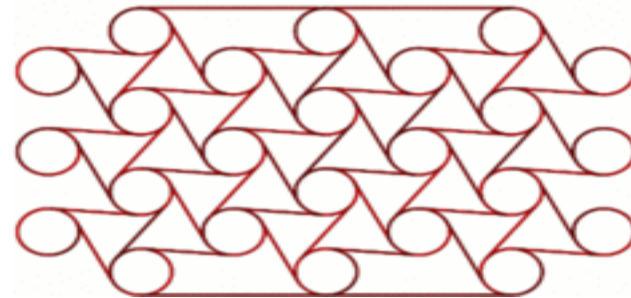
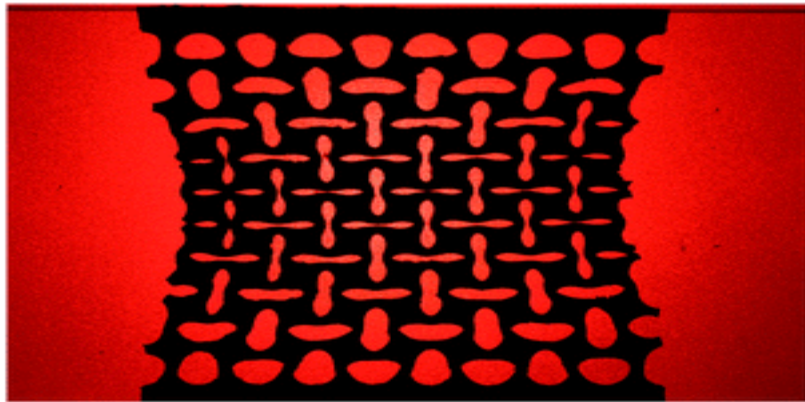
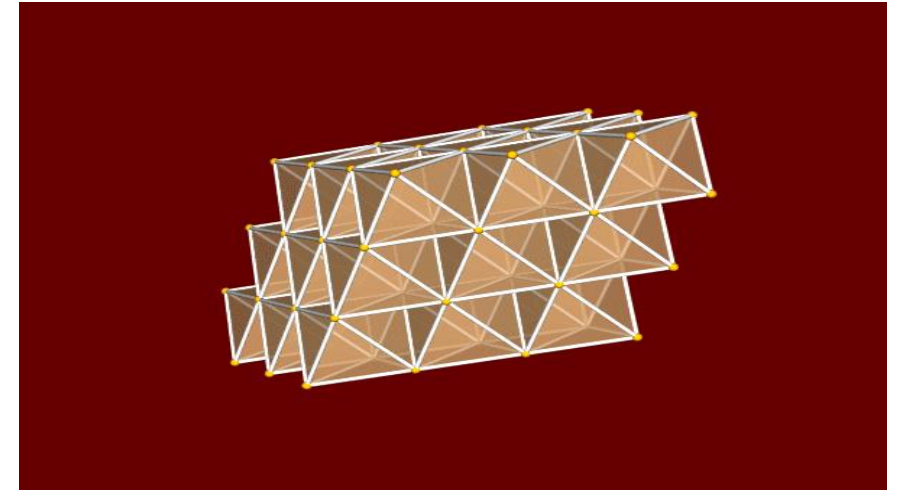
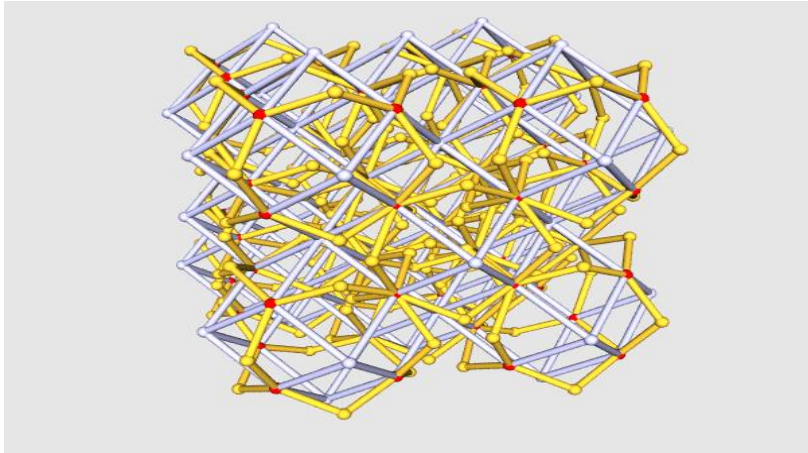
Explained and created by microstructures

Interesting applications

Auxetic material = αυξητικό υλικό

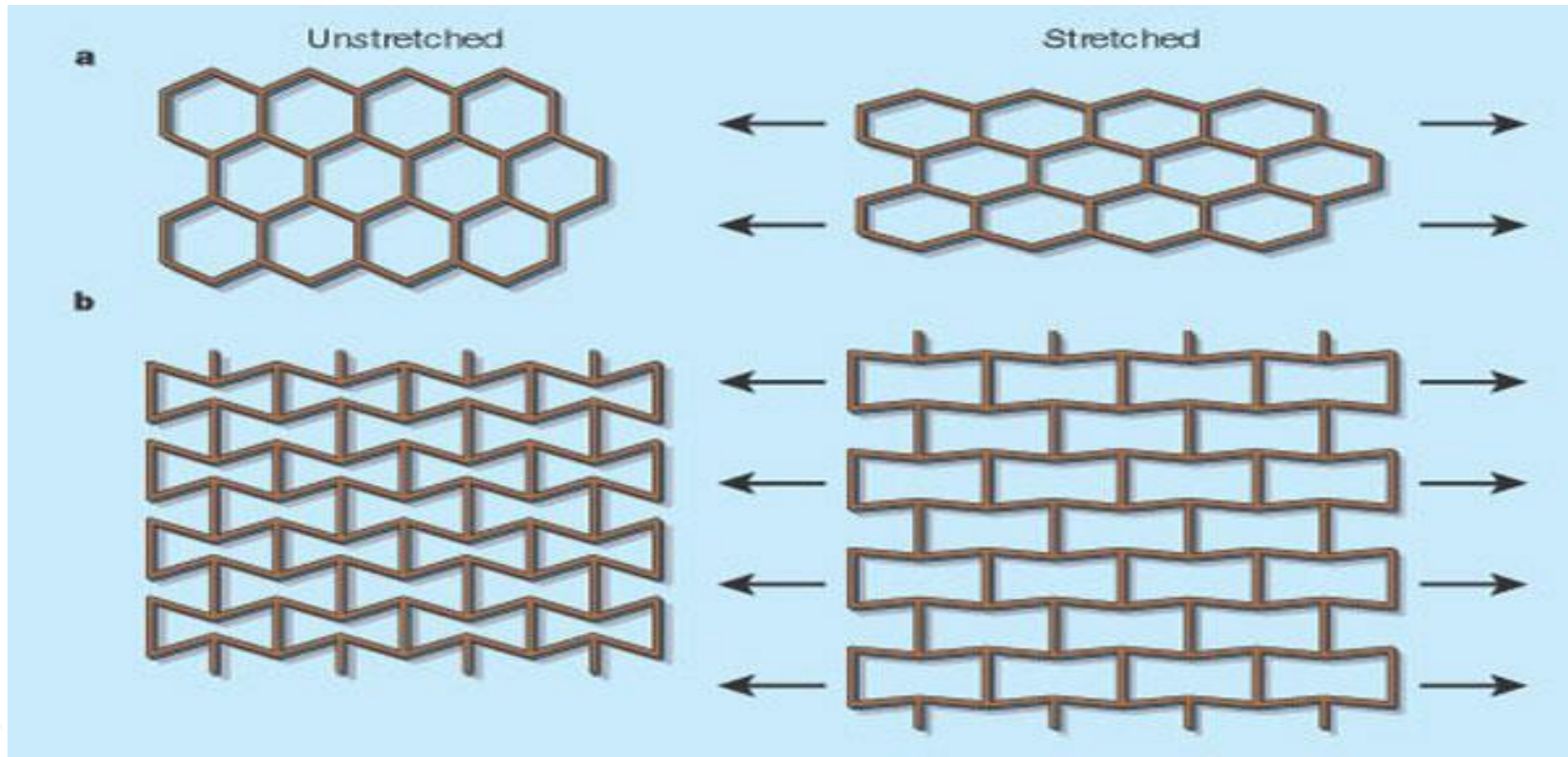


Auxetic mechanisms



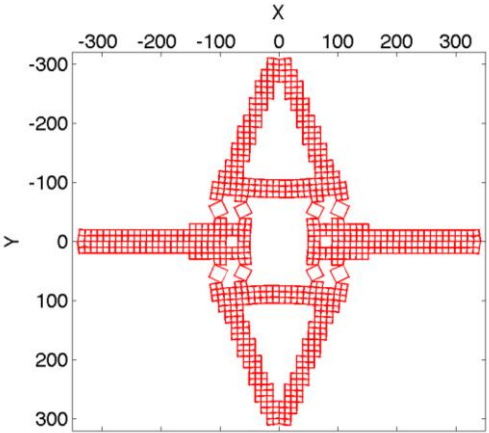
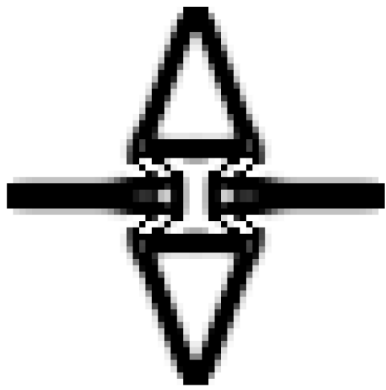
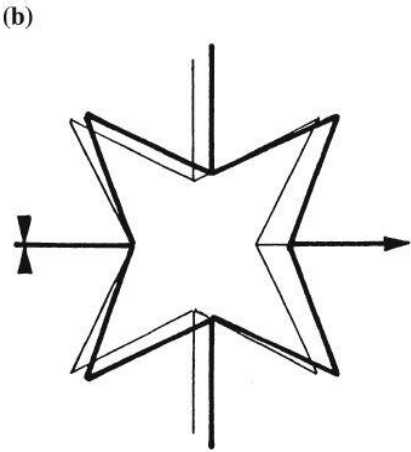
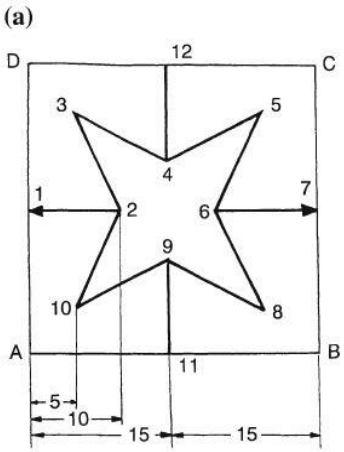
Auxetic Material

- Negative Poisson's ratio



Topology Optimization and Auxetic Microstructure

Auxetic microstructures lead to metamaterials with useful mechanical behaviour, in statics and dynamics. Beyond classical (e.g. star-shaped) microstructures, topology optimization gives much more flexibility.

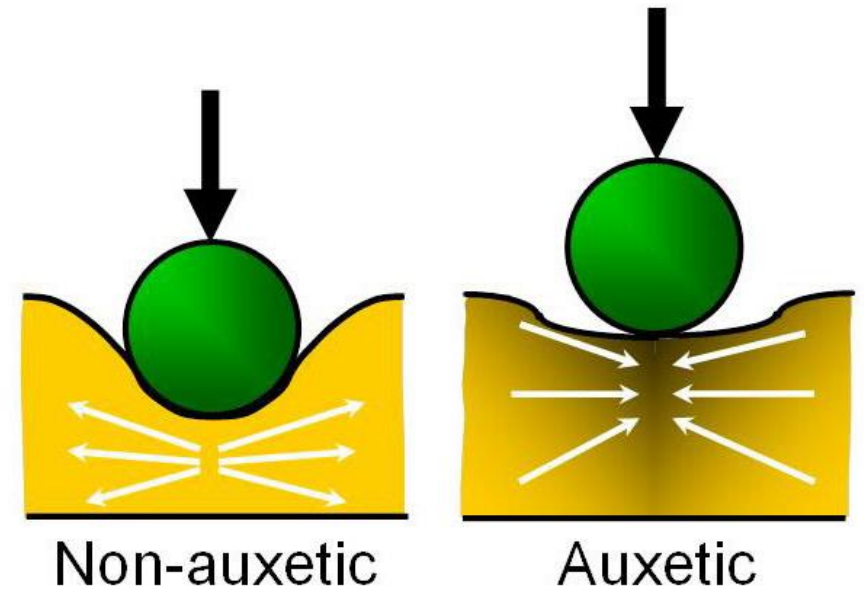
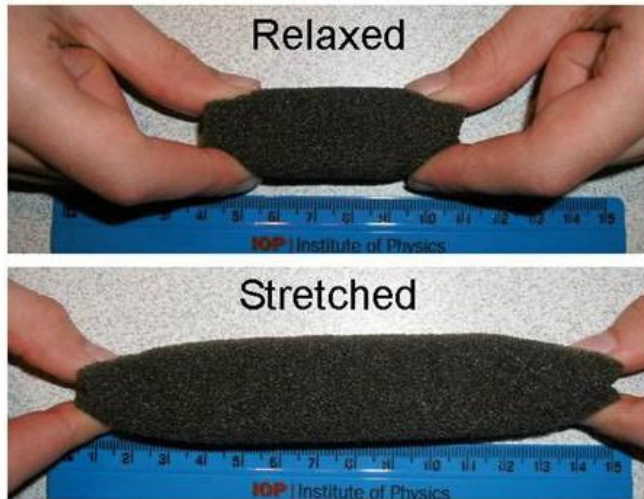


Source: Negative Poisson's ratios in composites with star-shaped inclusions: a numerical homogenization approach. Theocaris, P.S., Stavroulakis, G.E. & Panagiotopoulos, P.D. *Archive of Applied Mechanics* **67**, 274–286 (1997)

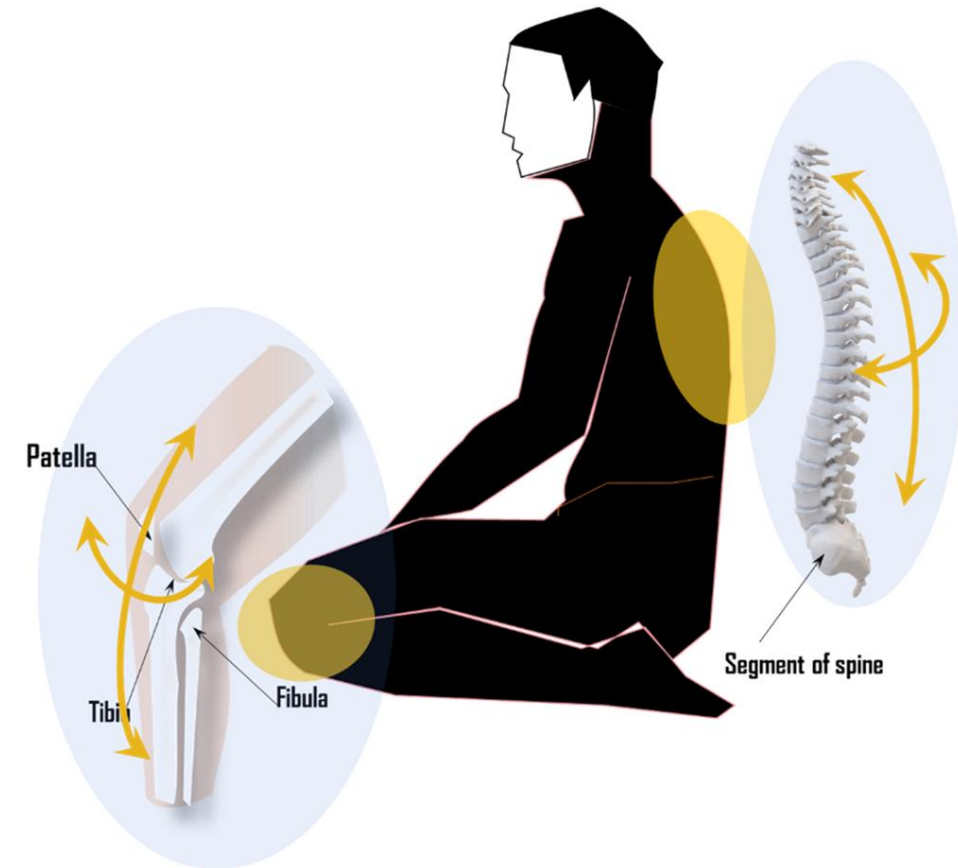
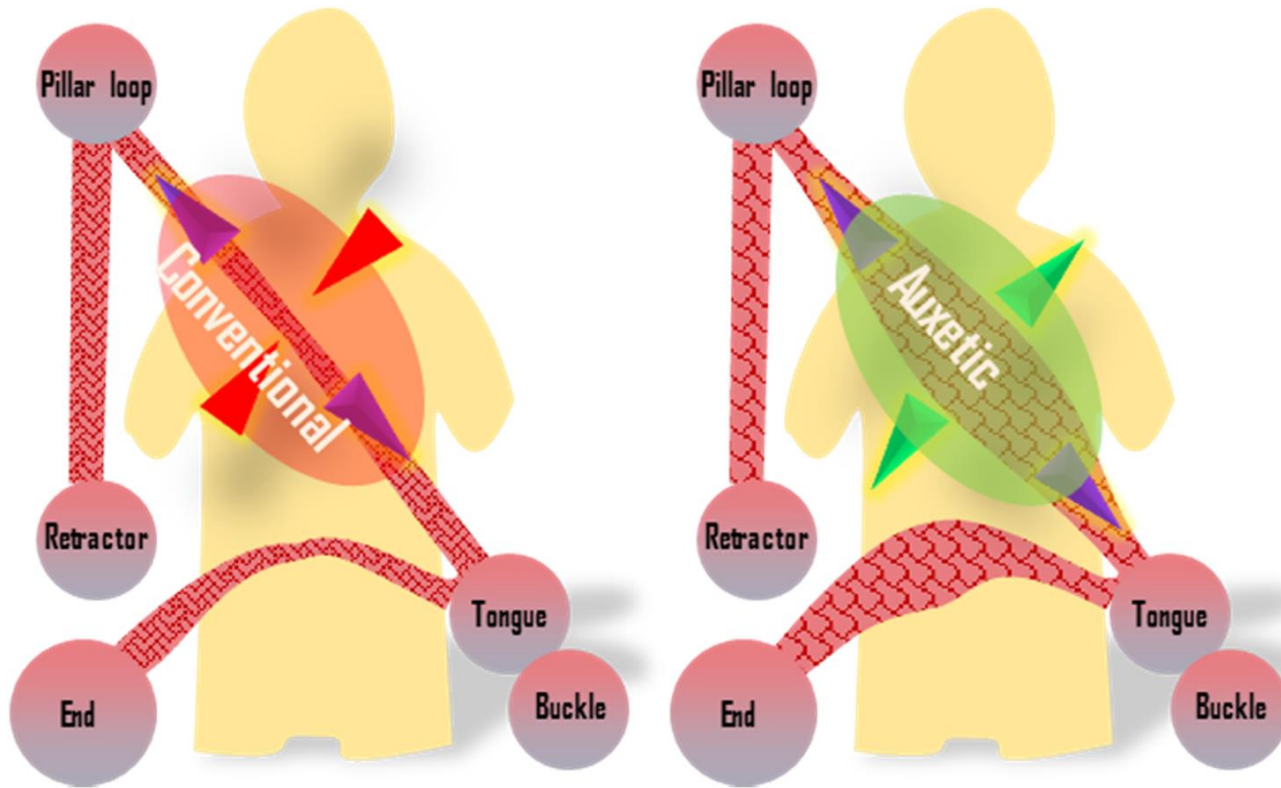
Source: Topology optimization for compliant mechanisms, using evolutionary-hybrid algorithms and application to the design of auxetic materials, N. Kaminakis, G.E. Stavroulakis, 2012
Kaminakis, PhD, TUC 2013



Properties of auxetics

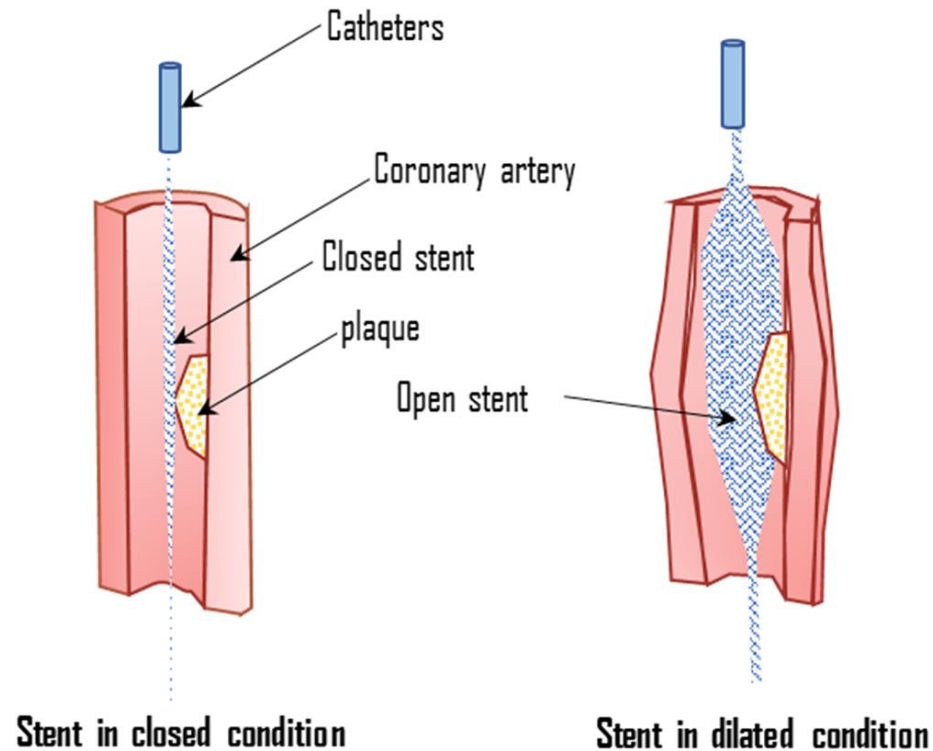


Auxetic applications: protection

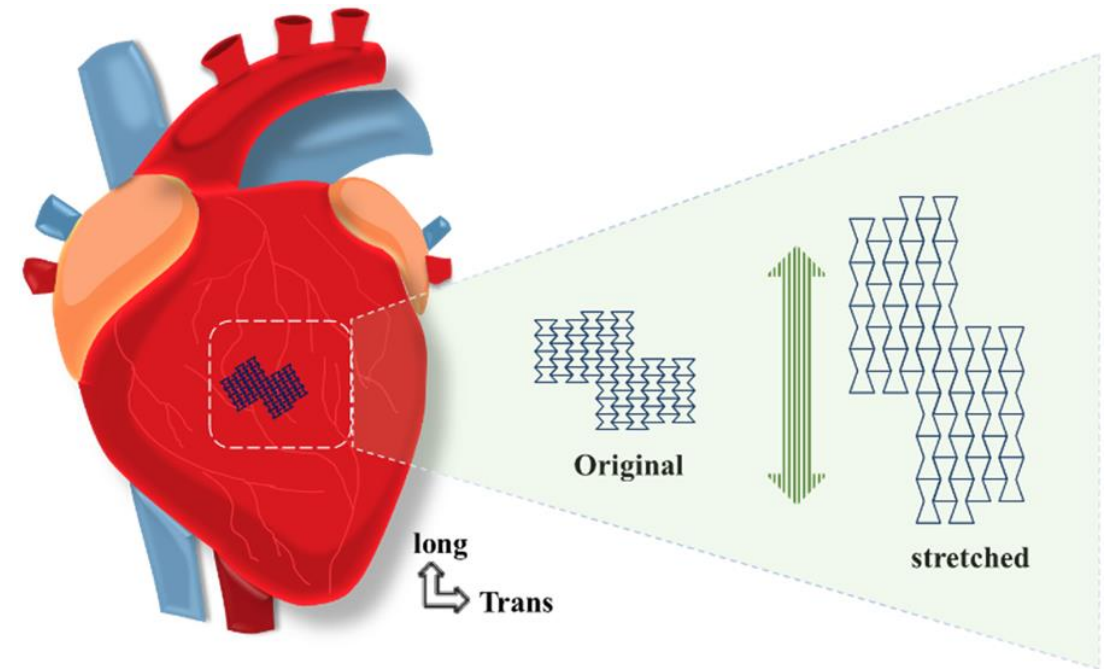


Auxetic mechanical metamaterials and their futuristic developments: A state-of-art review. Madhu Balan P , Johnney Mertens A , M V A Raju Bahubalendruni Materials Today Communications 34 (2023) 105285

Auxetic applications: biomechanics



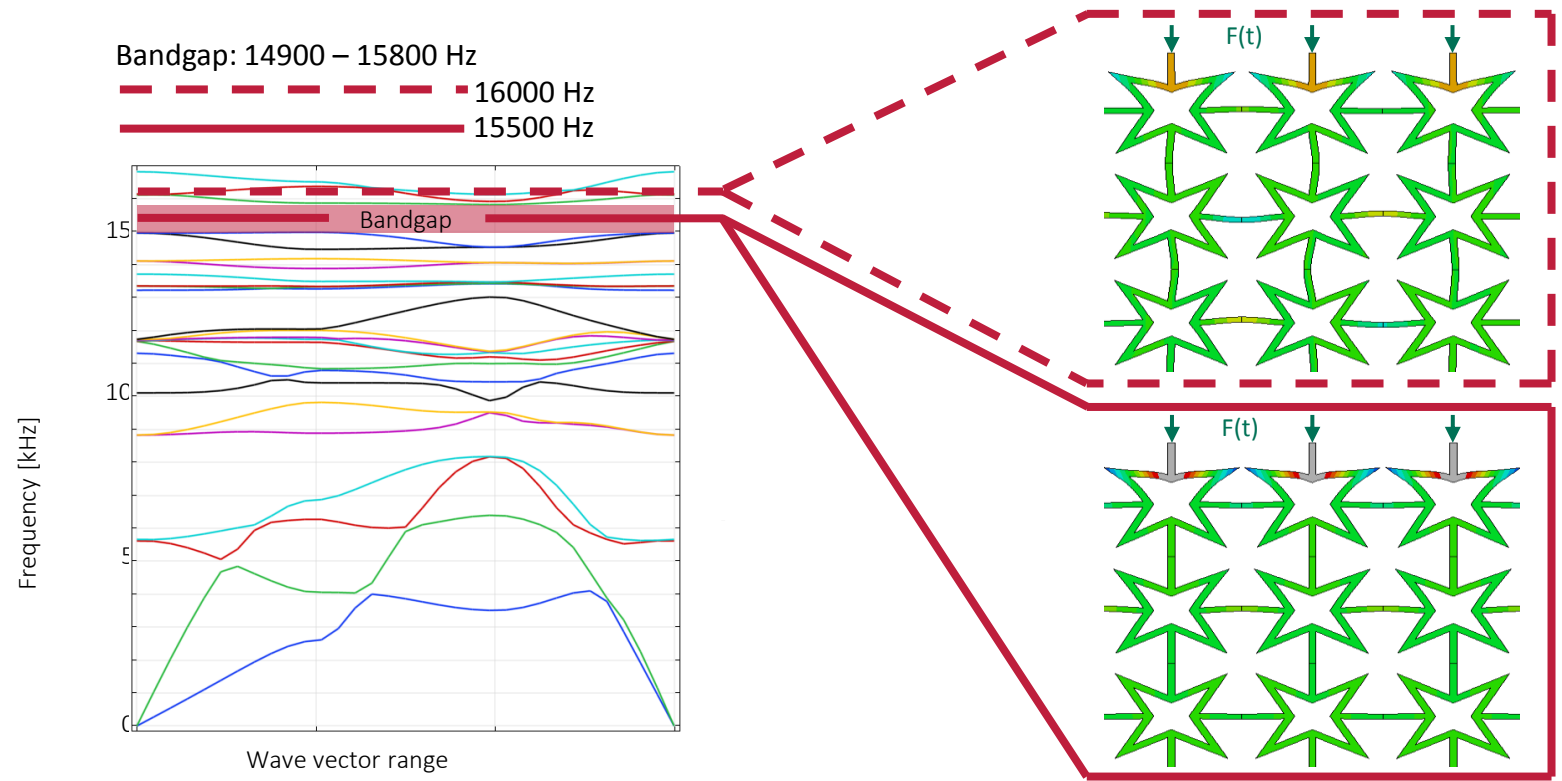
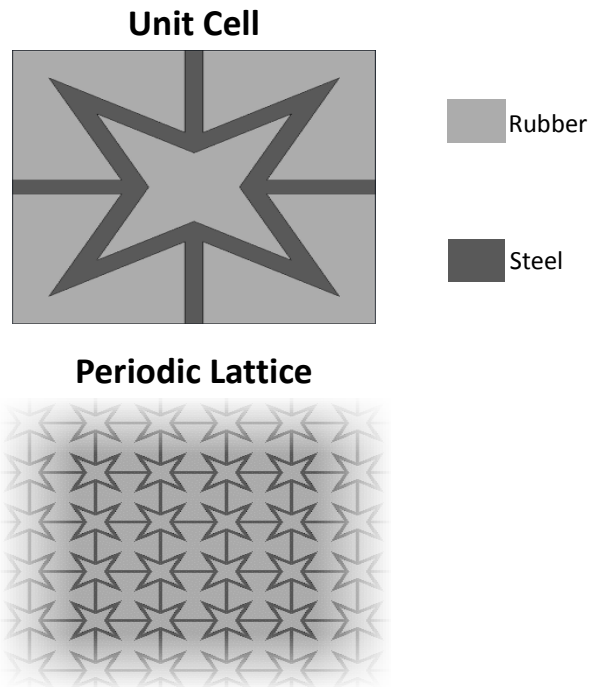
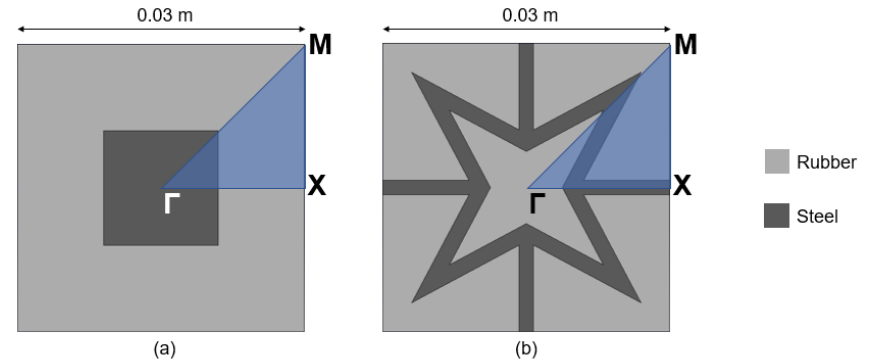
Auxetic stents



Auxetic cardiac patches

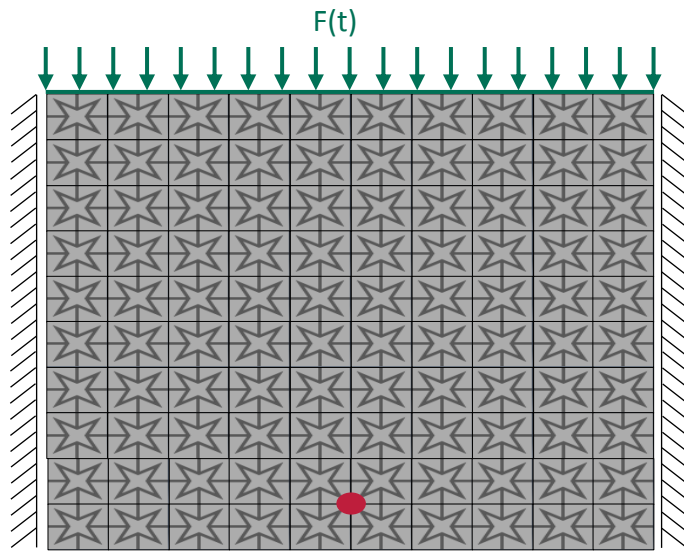
Auxetic mechanical metamaterials and their futuristic developments: A state-of-art review. Madhu Balan P , Johnney Mertens A , M V A Raju Bahubalendruni Materials Today Communications 34 (2023) 105285

Band gaps with Auxetics

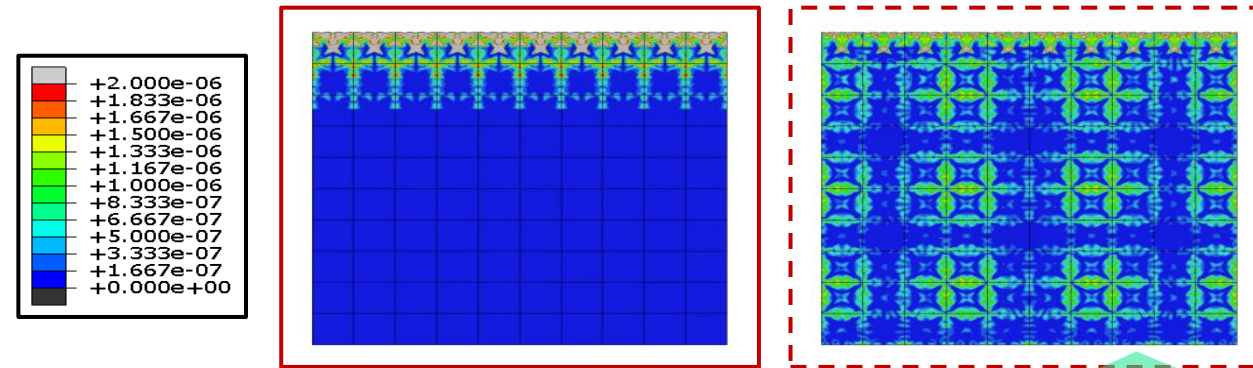
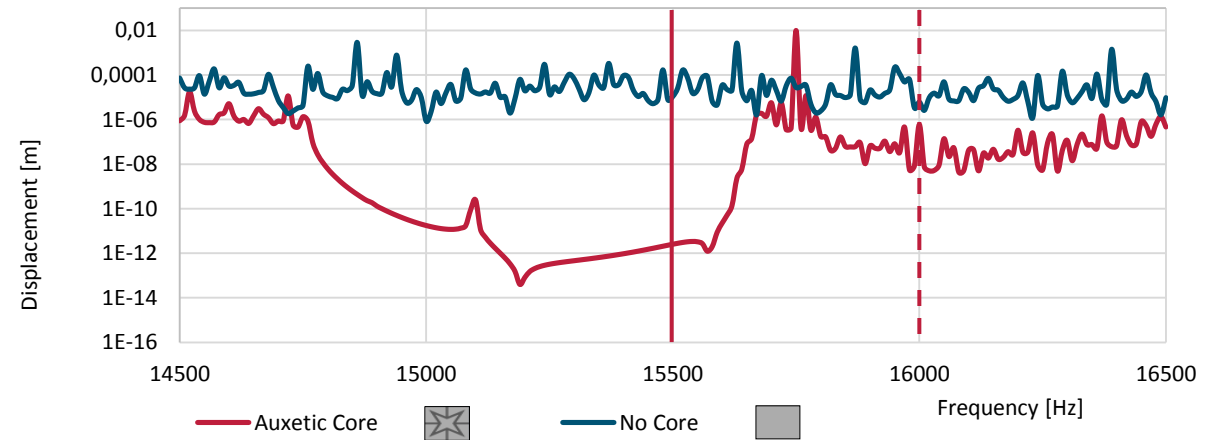


M. Rechenberg, Bachelor Thesis, TU Braunschweig, 2020, P. Koutsianitis PhD, TUC, 2020
 P.I. Koutsianitis, G.K. Tairidis, G.A. Drosopoulos, G.E. Stavroulakis. Conventional and star-shaped auxetic materials for the creation of band gaps. *Archive of Applied* 89 (12), 2545-2562, 2019.

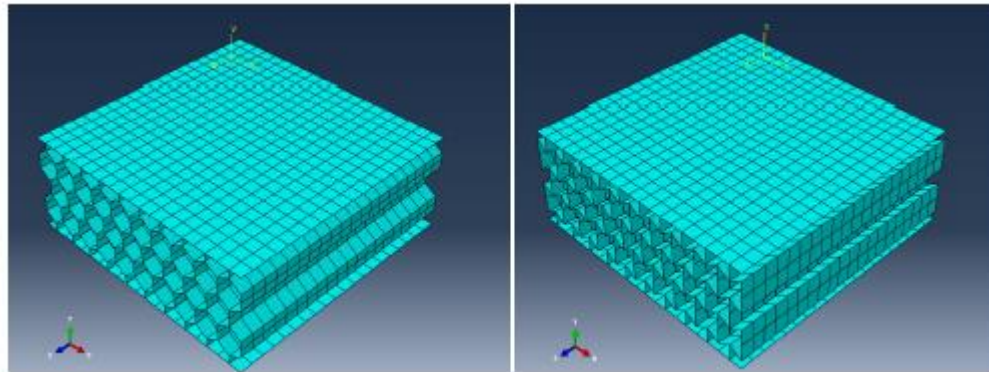
Band gaps with Auxetics



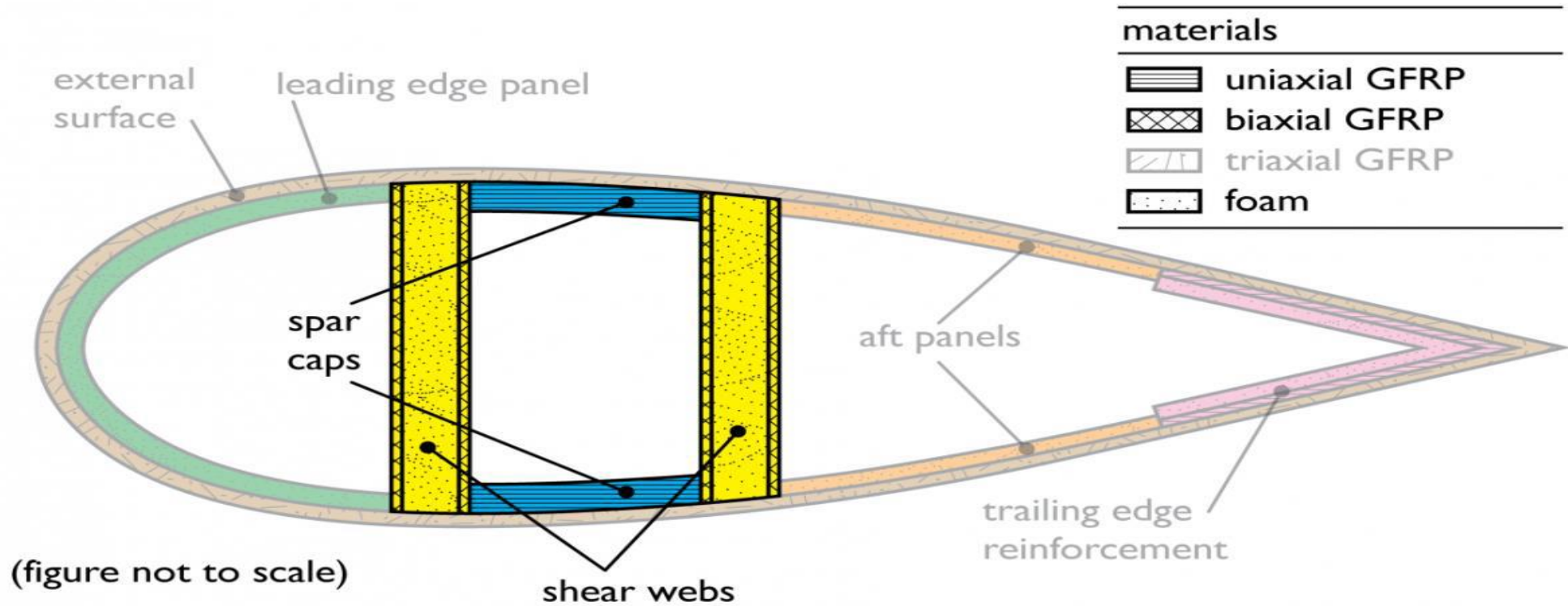
- 10 by 10 auxetic unit cells
- Harmonic pressure load on top core surface
- Oscillations measured at the bottom ()



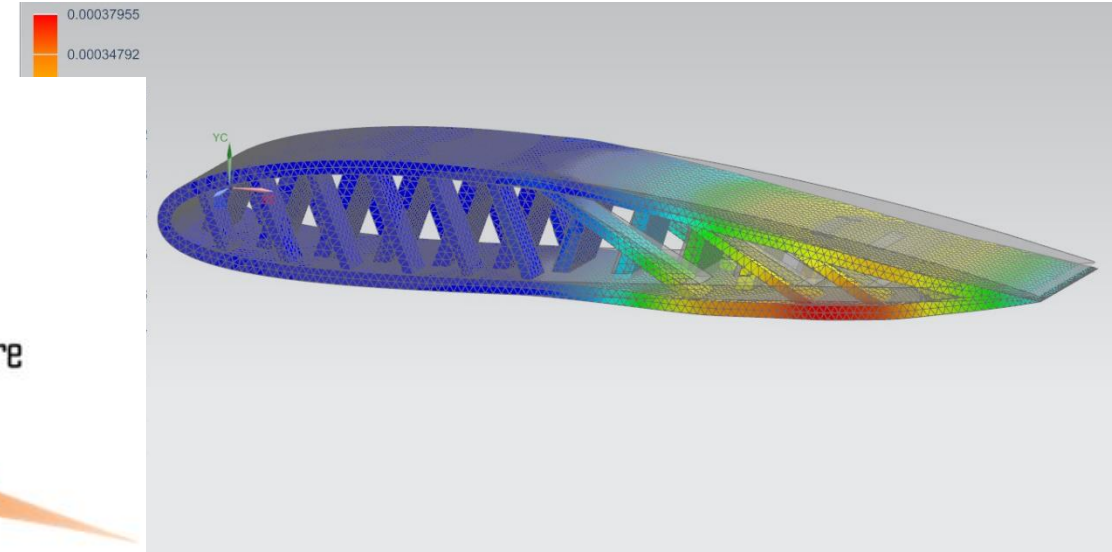
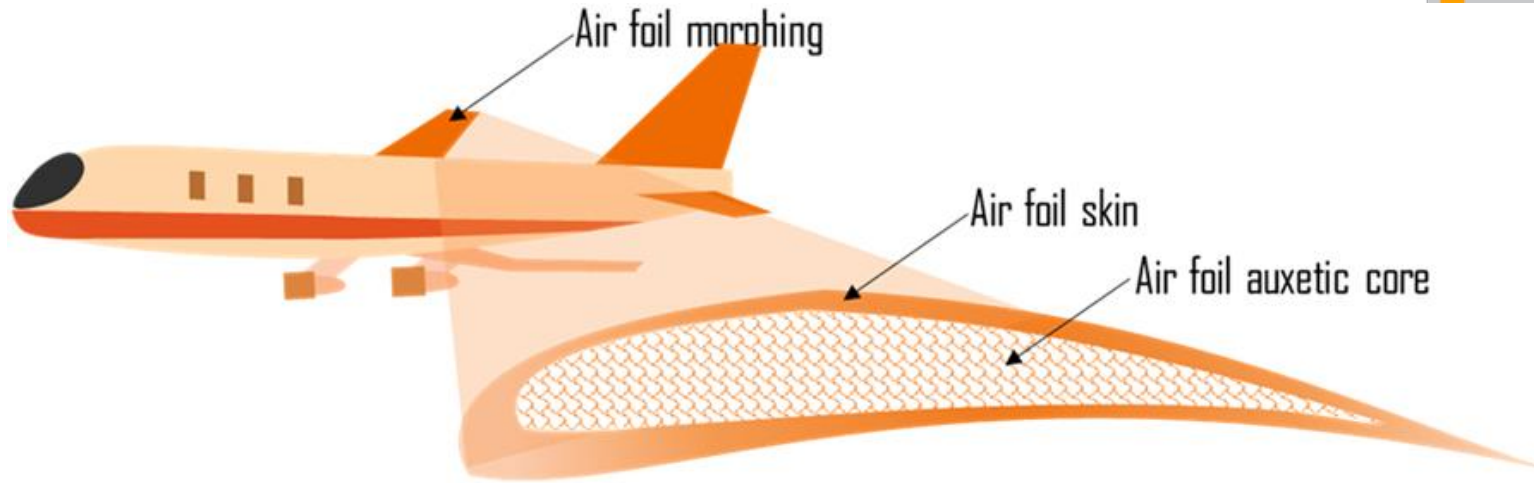
Application on vibration-isolation at high-speed boat



Auxetic isolation for wind turbine blades



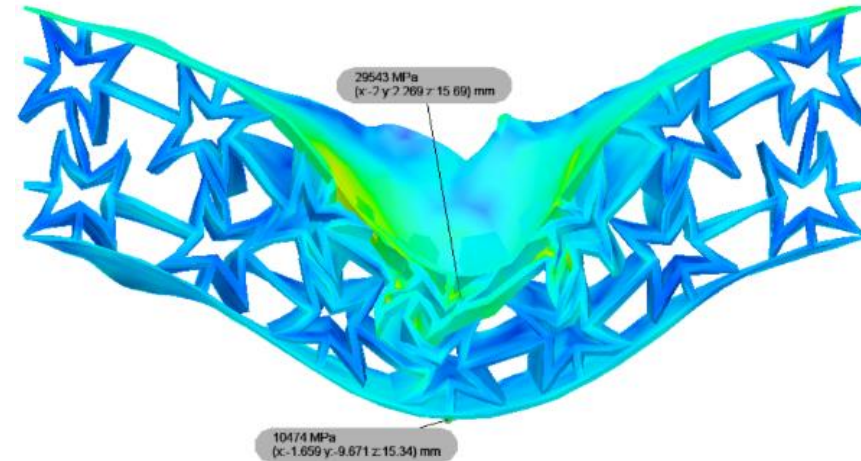
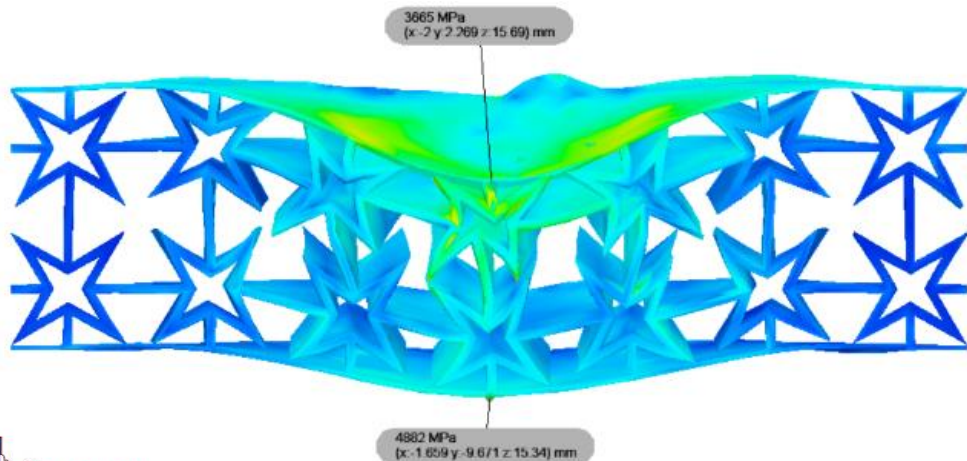
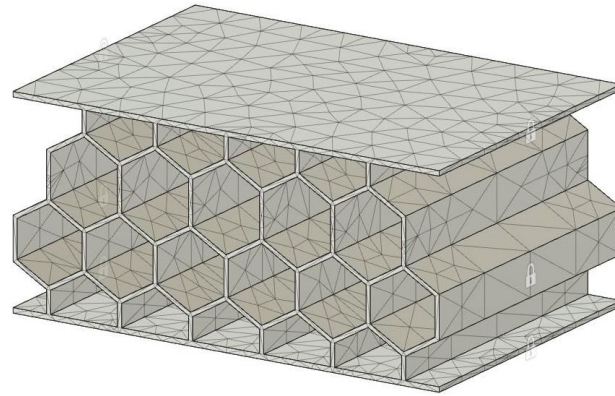
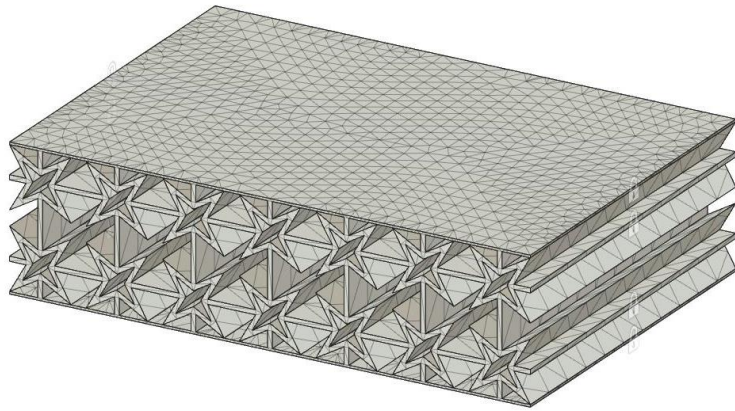
Morphing of blades



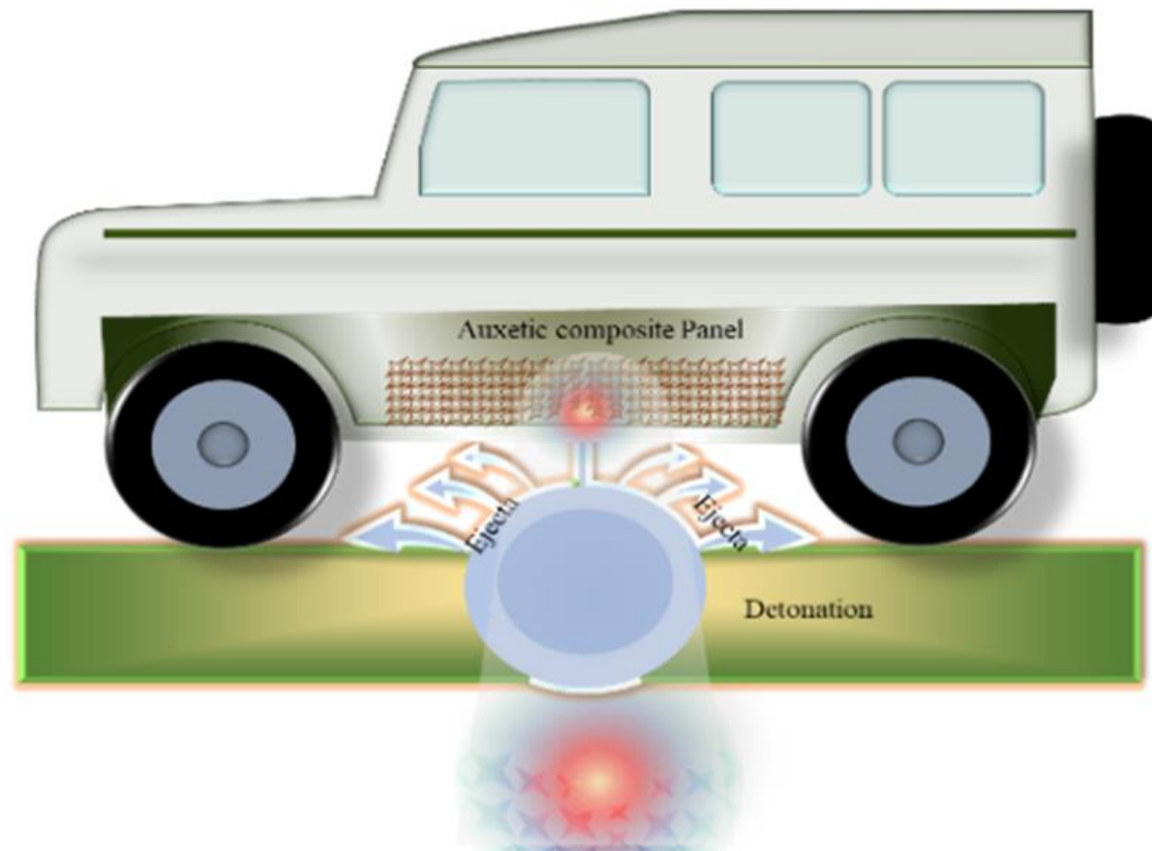
D. Vokas, Diploma Thesis TUC 2019

Auxetic mechanical metamaterials and their futuristic developments: A state-of-art review. Madhu Balan P , Johnney Mertens A , M V A Raju Bahubalendruni Materials Today Communications 34 (2023) 105285

Bullet penetration in an auxetic plate

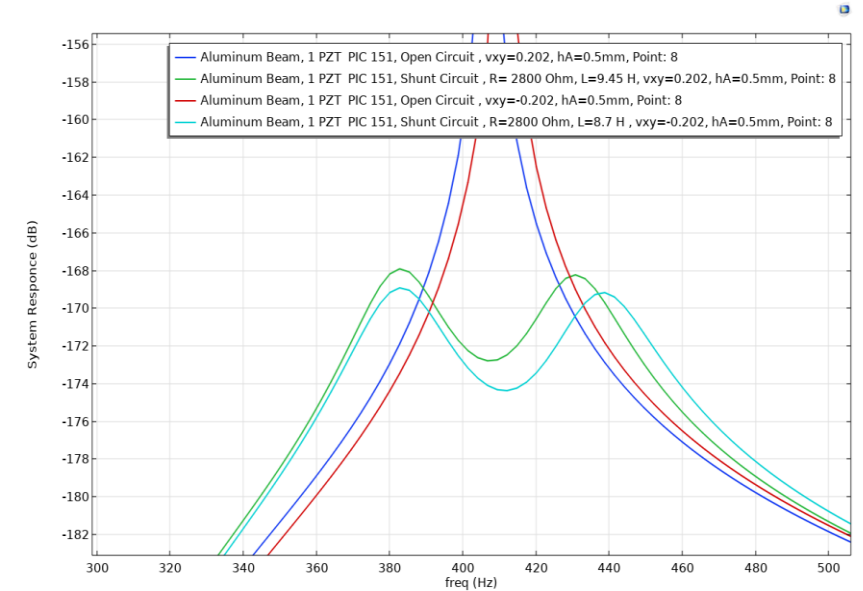
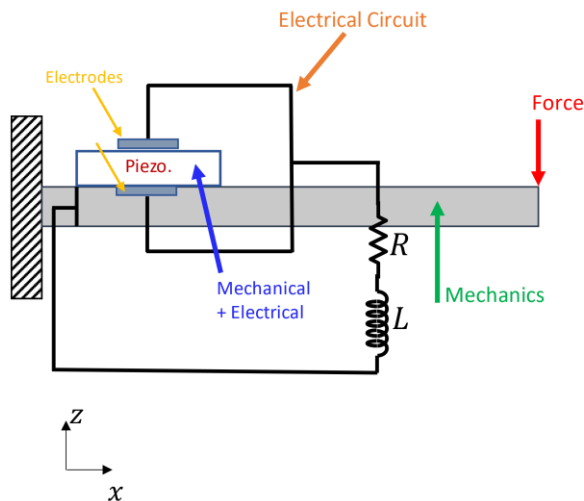
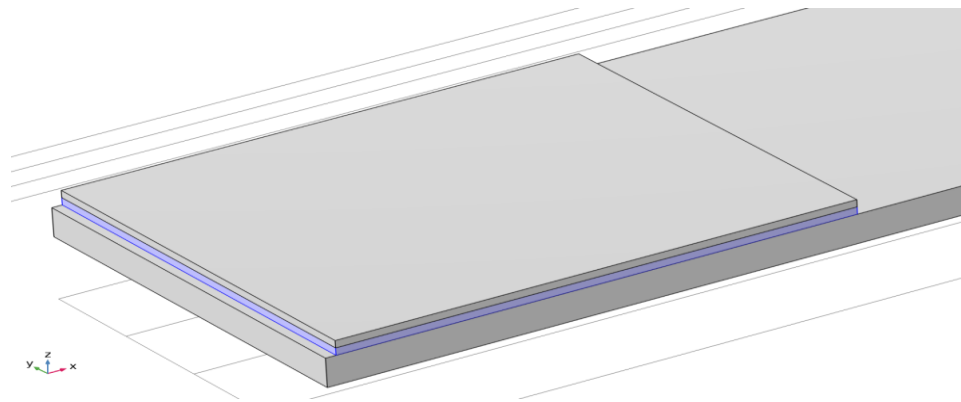


Auxetic armour protection of vehicles



Auxetic mechanical metamaterials and their futuristic developments: A state-of-art review. Madhu Balan P , Johnney Mertens A , M V A Raju Bahubalendruni Materials Today Communications 34 (2023) 105285

Auxetic enhancement of shunted piezoelectrics



Modeling of shunted piezoelectrics and enhancement of vibration suppression through an auxetic interface, Micromachines 2023

Maria-Styliani Daraki, Konstantinos Marakakis and Georgios E. Stavroulakis

K. Marakakis, PhD, TUC, 2022

Nike patented auxetic soles

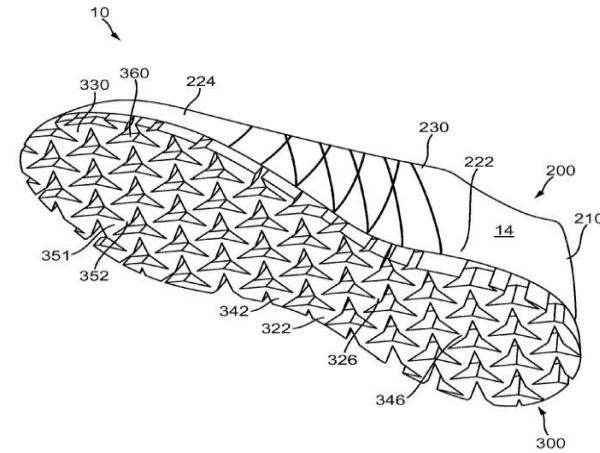
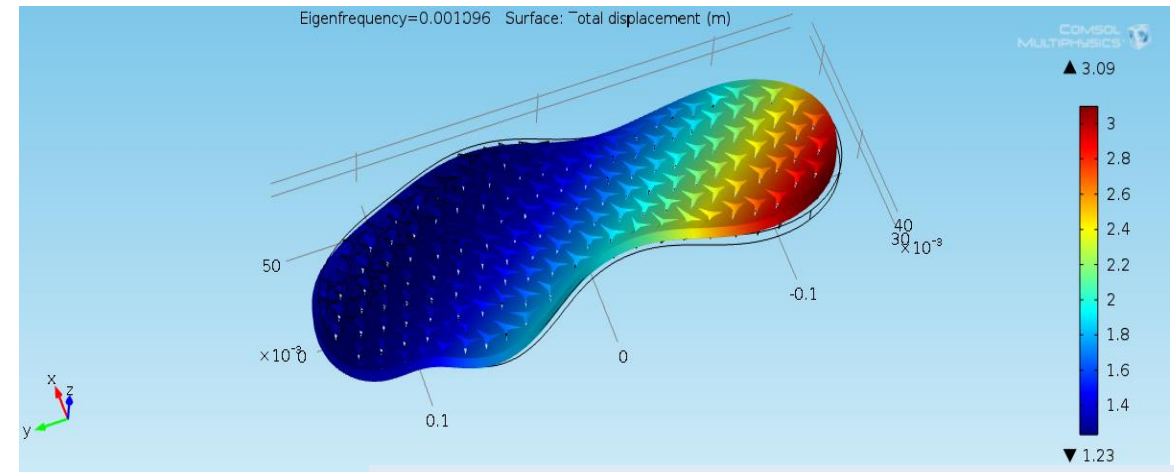
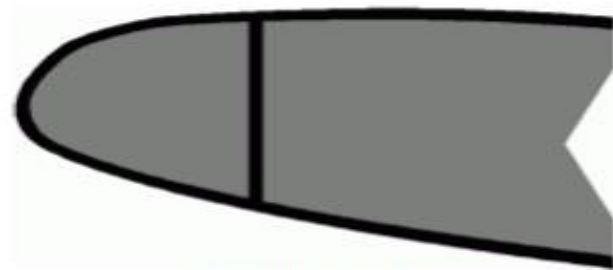


FIG. 3

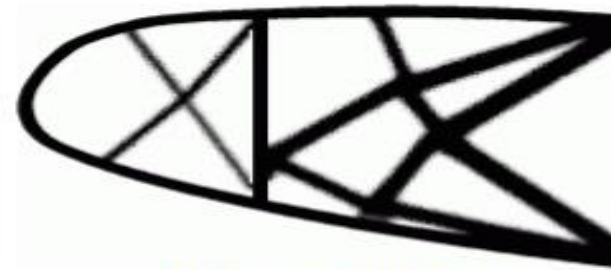


P. Boura, Master Thesis, TUC 2016

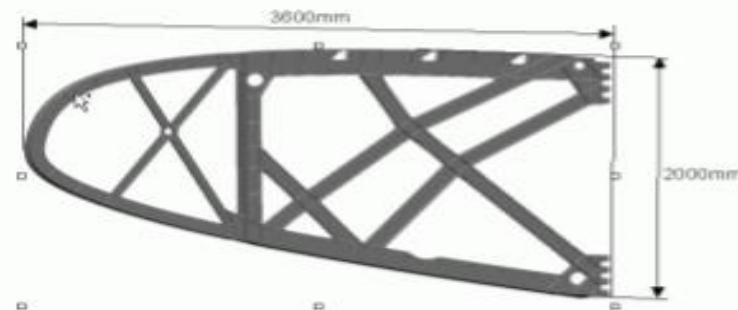
Topology Optimization



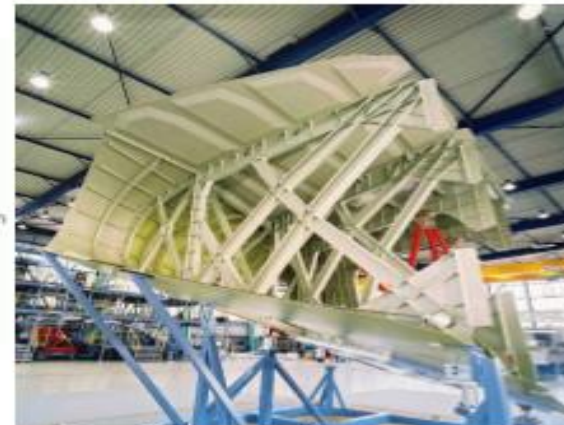
Design domain



Optimized topology



Actual structure



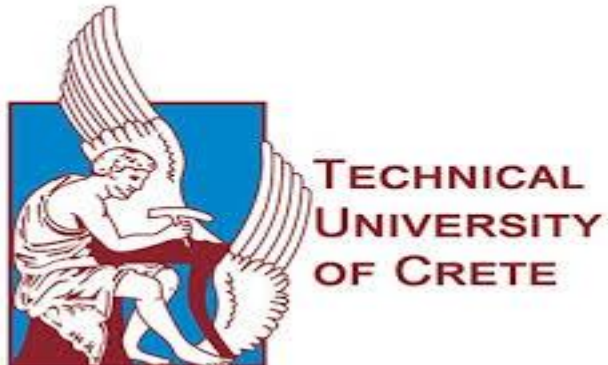
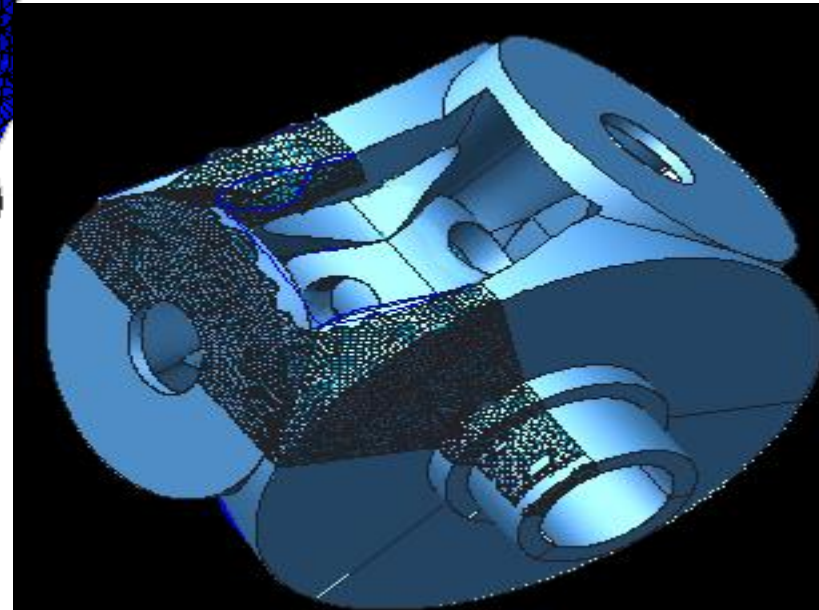
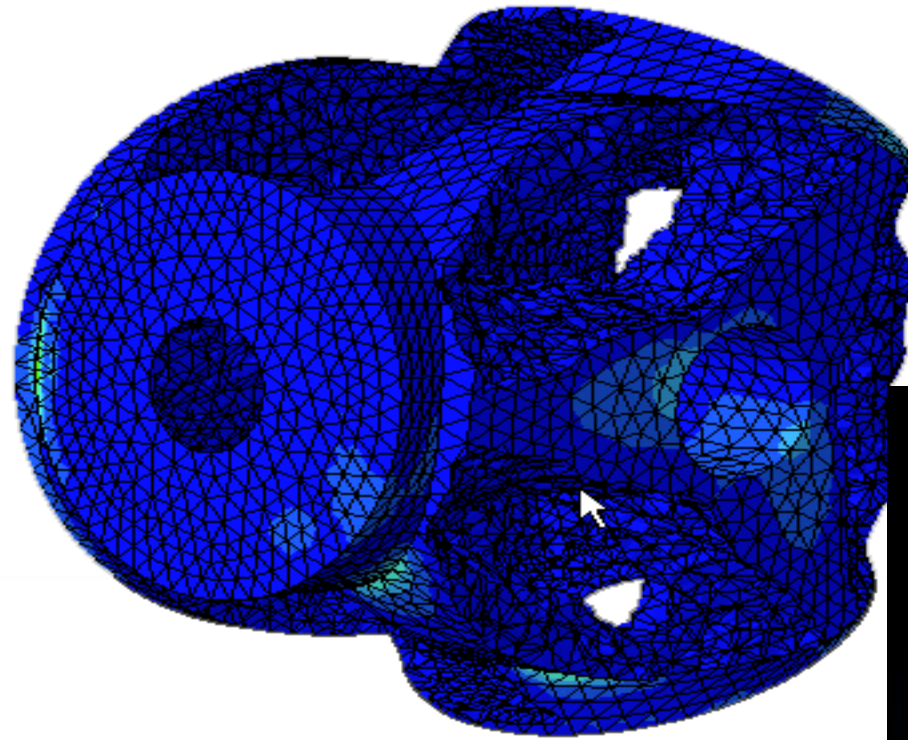
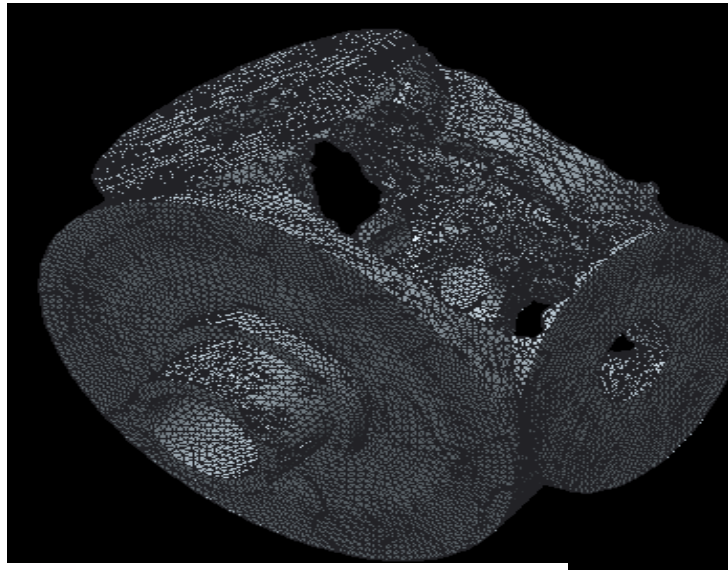
Manufactured wing structure



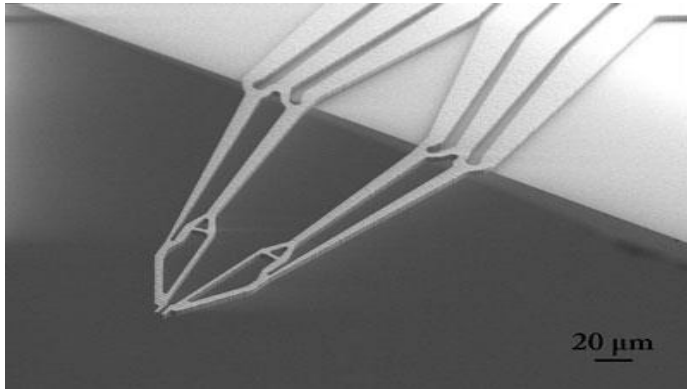
TECHNICAL
UNIVERSITY
OF CRETE

A structural part of the A380 aircraft of Airbus

Topology optimization of a rotor, in a wind turbine



Topology Optimization Mechanisms



Nanomechanics Gripper (Image: *Özlem Sardan, DTU, www.nanohand.eu*)

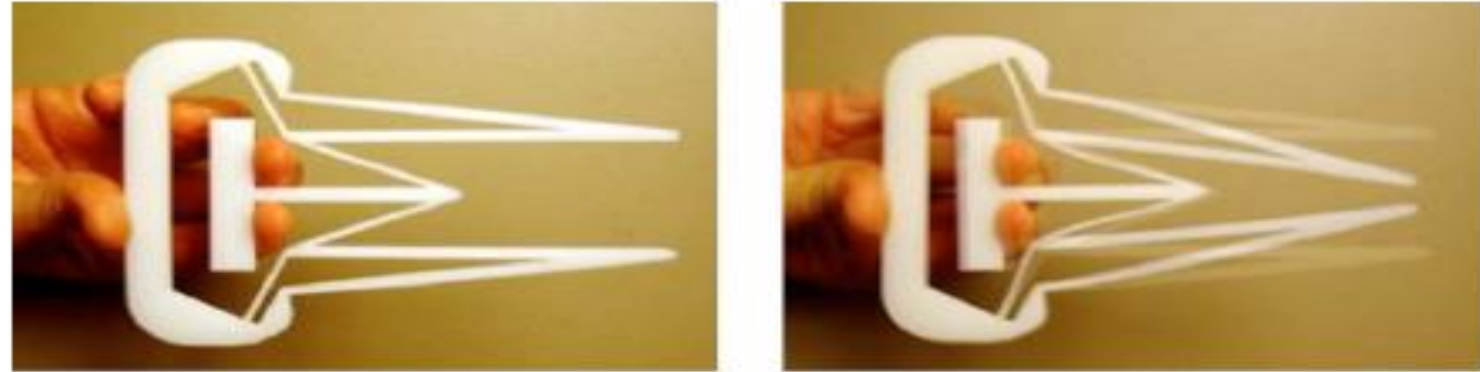
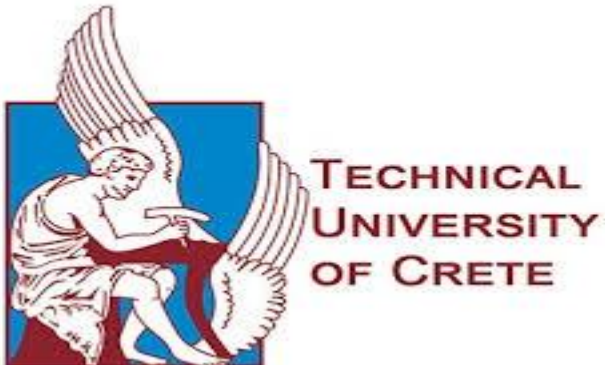


Fig. 7 Prototype of the compliant gripper in its inactive mode (left) and gripping mode (right)

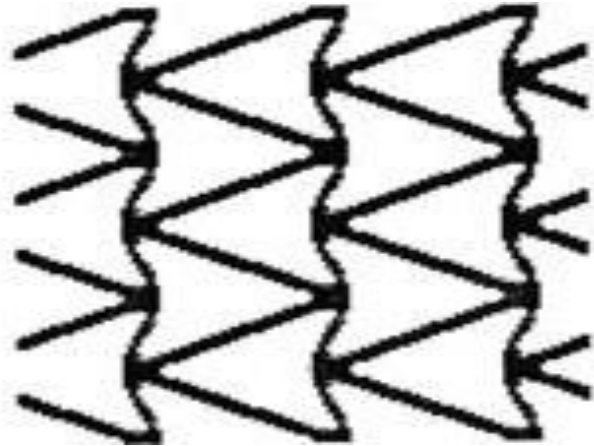
Mechanical Gripper modelled as a Compliant mechanism.



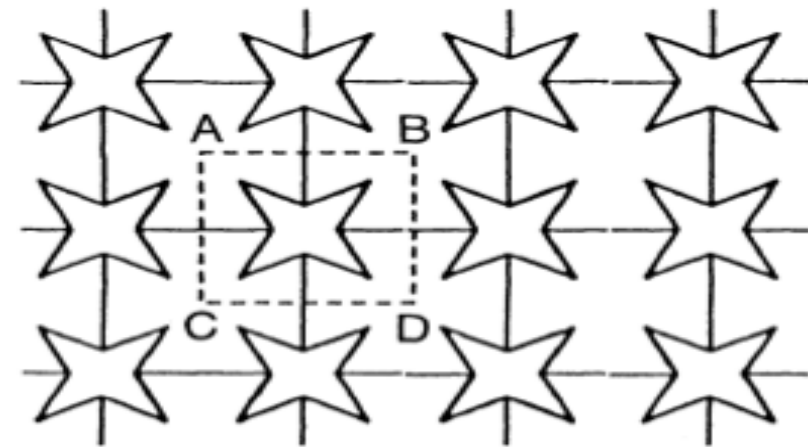
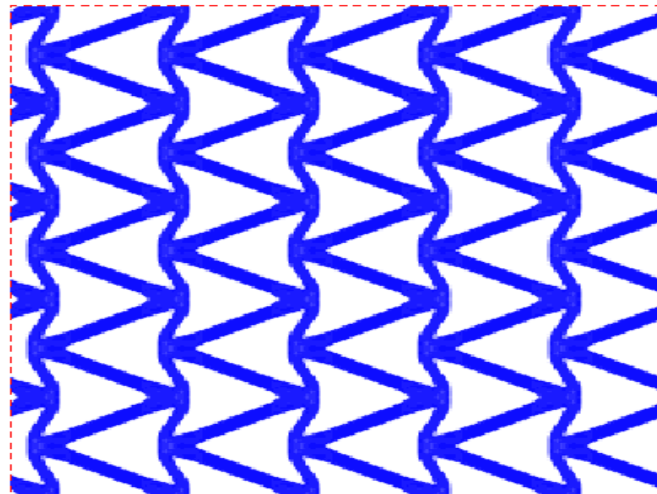
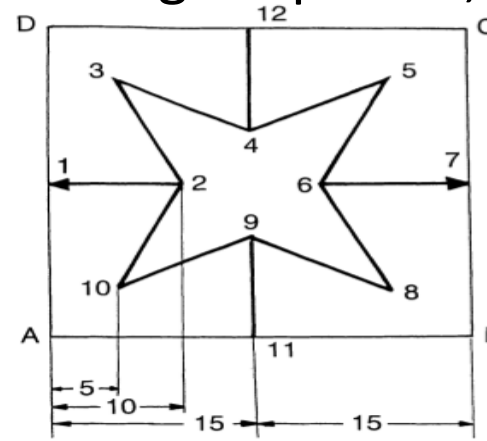
Auxetic Material

Previous works (based on flexible microstructures)

- Larsen et al, 1997



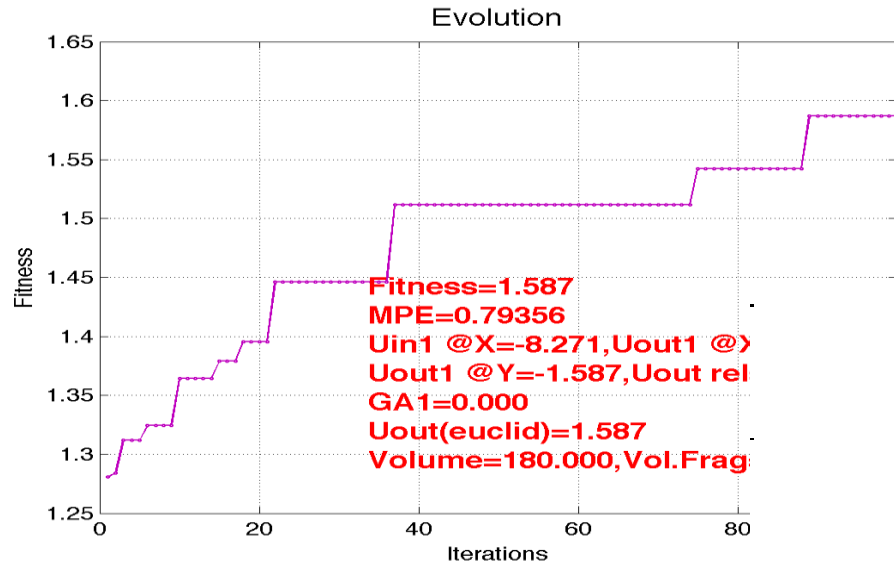
- Theocharis, Stavroulakis, Panagiotopoulos, 1997



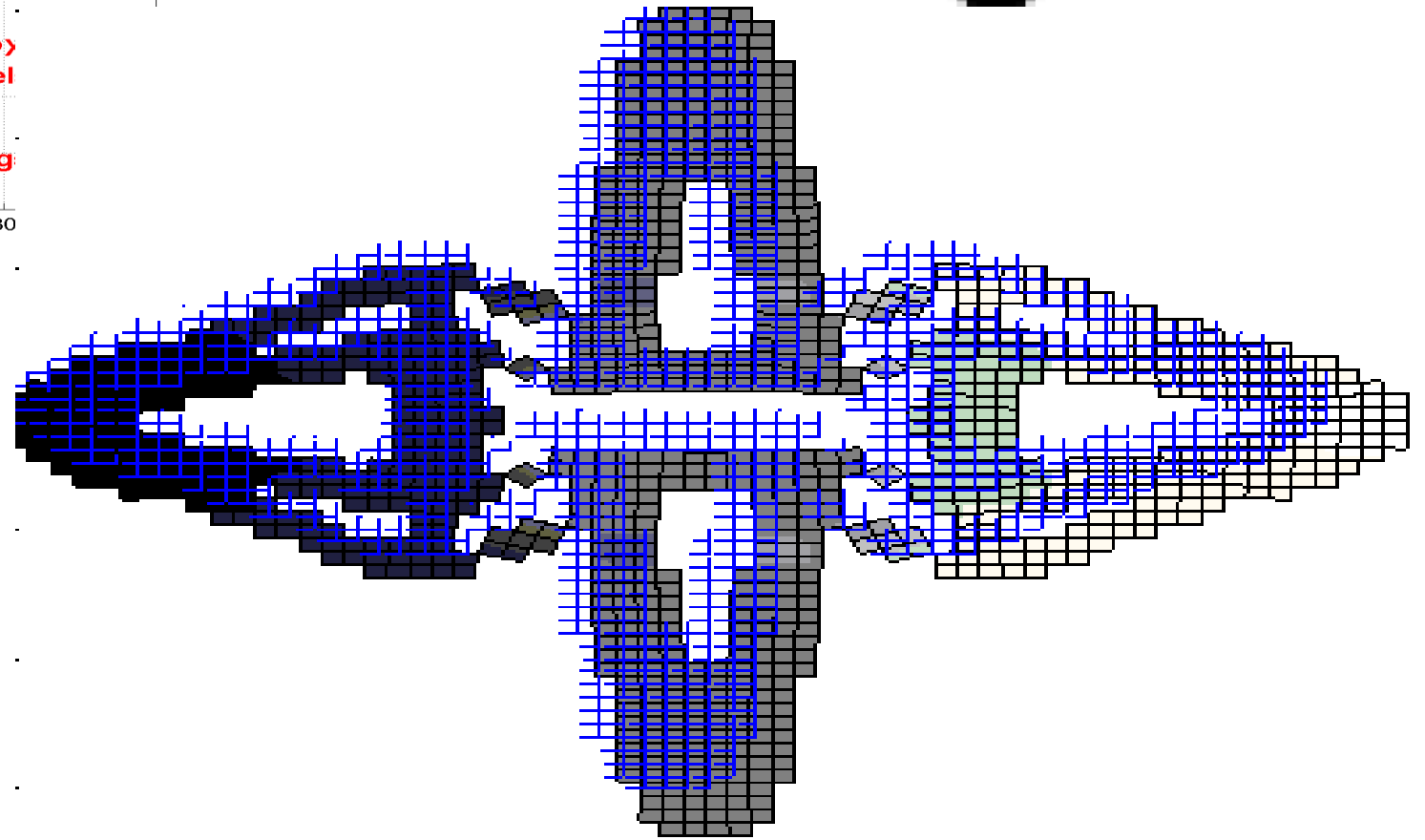
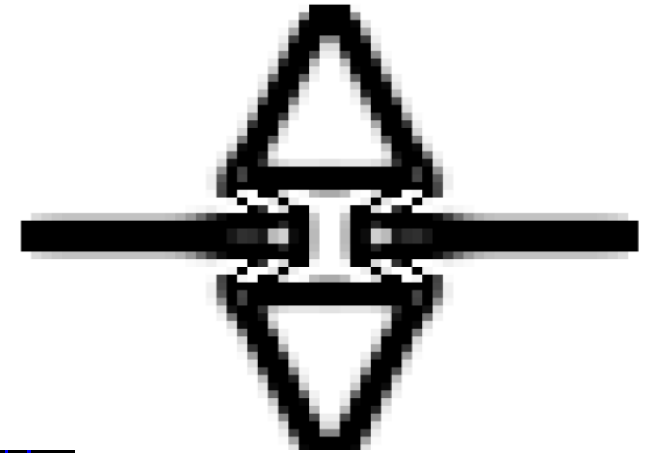
TECHNICAL
UNIVERSITY
OF CRETE

Continuous formulation

30x30 elements, Volume fraction: :



$$\text{Poissons Ratio} = -\frac{-1.587}{-8.271} = -0,192$$



TECHNICAL
UNIVERSITY
OF CRETE

Optimization problem for band gap analysis

Objective Function

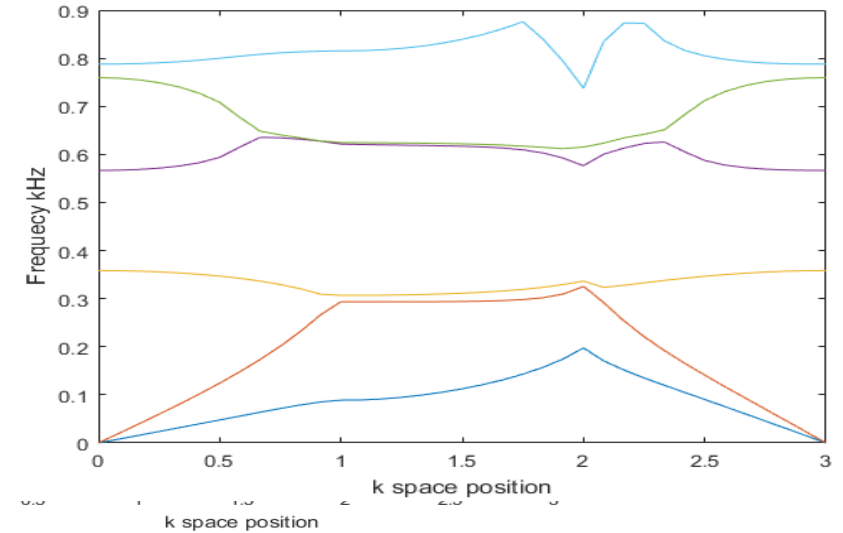
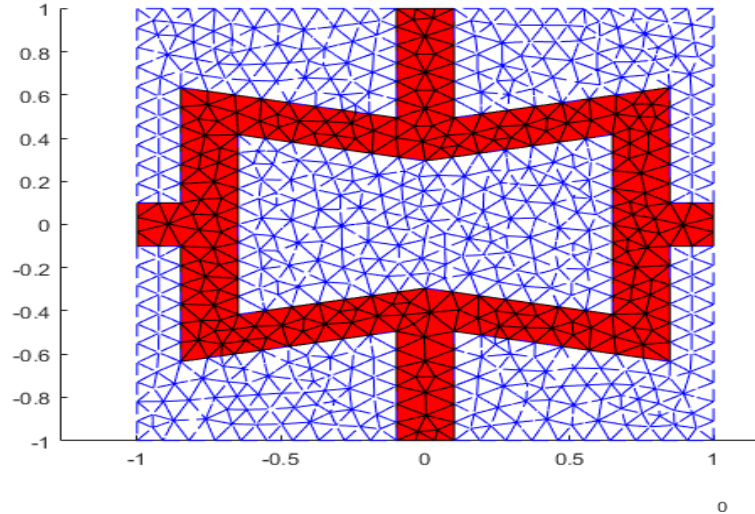
Maximize the Band Gap Area

Constraints

Symmetry design constraints

e.g. at y axis: $n2 < 1$

at x axis: $n1 < 0$, etc.



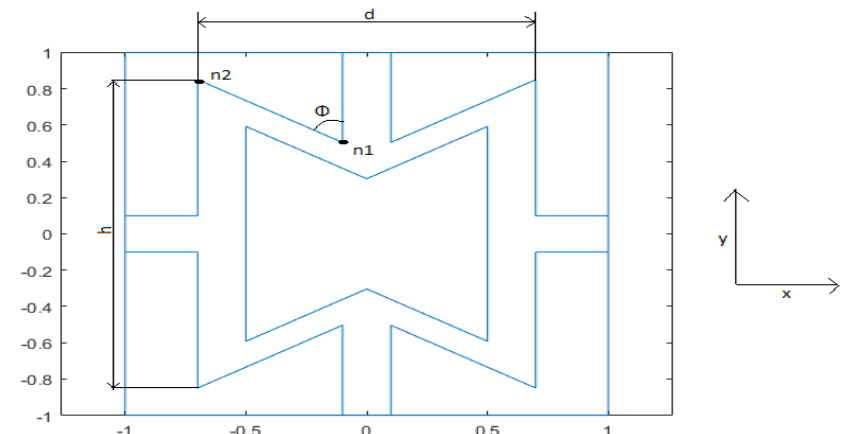
TECHNICAL
UNIVERSITY
OF CRETE

Design Variables:

Height: $h \in [0.2, 1.9]$

Width: $d \in [0.2, 1.9]$

Angle: $\Phi \in [50^\circ, 120^\circ]$



Microstructures: Analytic homogenization

Lead to homogenized mechanical properties (orthotropic etc)

Can be tailored (graded

Microstructures: Numerical homogenization

Lead to homogenized mechanical properties (orthotropic etc)

Can be tailored (graded materials, better than classical composites, suitable for AM)

In dynamics: band gap properties

Lead to mechanical metamaterials

Open questions: defects during construction, a lot of investigation related to 'missing ribs' etc

Technology limitations

Microstructures: Functionally graded

Lead to homogenized mechanical properties (orthotropic etc)

Can be tailored (graded materials, better than classical composites, suitable for AM)

In dynamics: band gap properties

Lead to mechanical metamaterials

Open questions: defects during construction, a lot of investigation related to 'missing ribs' etc

Technology limitations

Microstructures: Missing ribs etc

Lead to homogenized mechanical properties (orthotropic etc)

Can be tailored (graded materials, better than classical composites, suitable for AM)

In dynamics: band gap properties

Lead to mechanical metamaterials

Open questions: defects during construction, a lot of investigation related to 'missing ribs' etc

Technology limitations

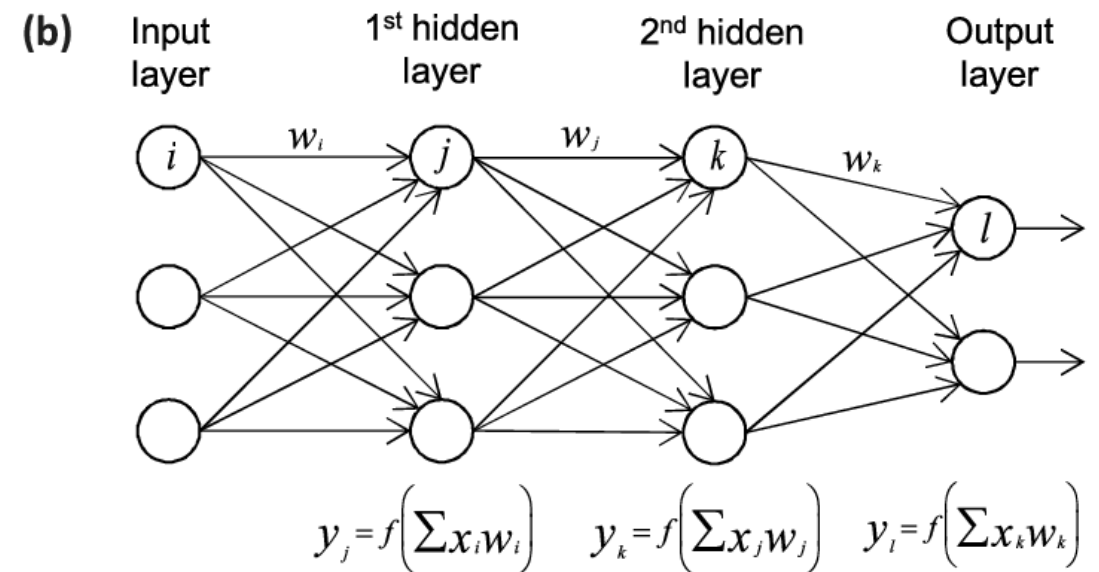
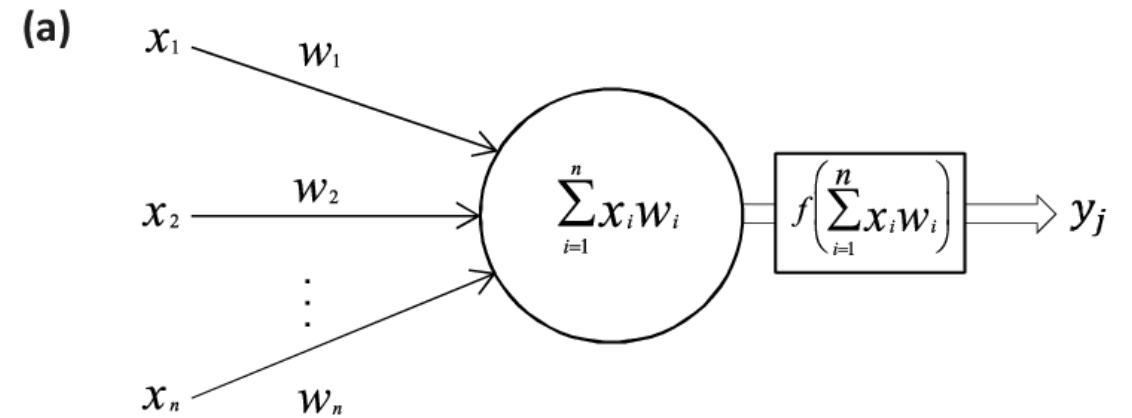
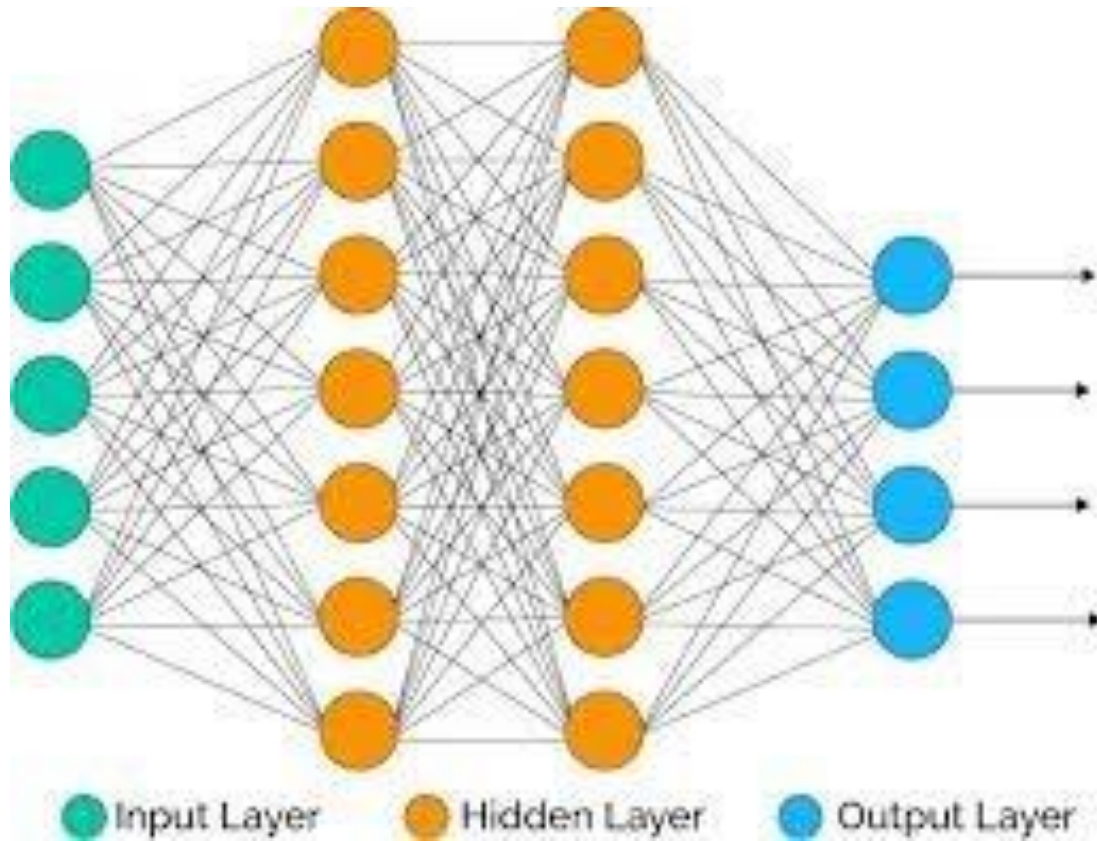
Models vs Data

- Models have concrete mathematical structure
- Models allow for classical approximation
- Data are uncorrelated quantities
- Data require processing and possibly extraction of knowledge
- Hybrid scheme: integrate within a model data
- Example: material relations in Finite Elements

Neural networks, Deep Learning, Artificial Intelligence, Big Data Analytics

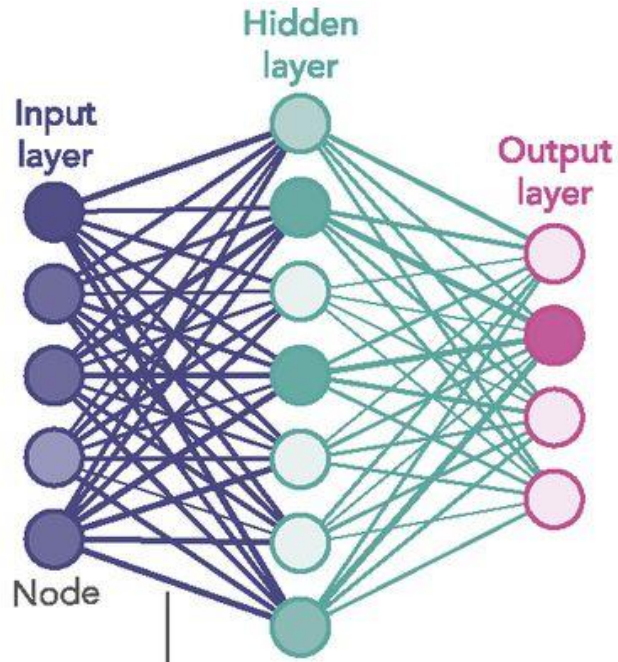
- Model-free estimators
- Exploitation of big data, from experiments or numerical simulation
- Suitable for: direct analysis (replacement of material constitutive law), inverse analysis (structural health monitoring)
- Next step: Digital Twin

Backpropagation NN



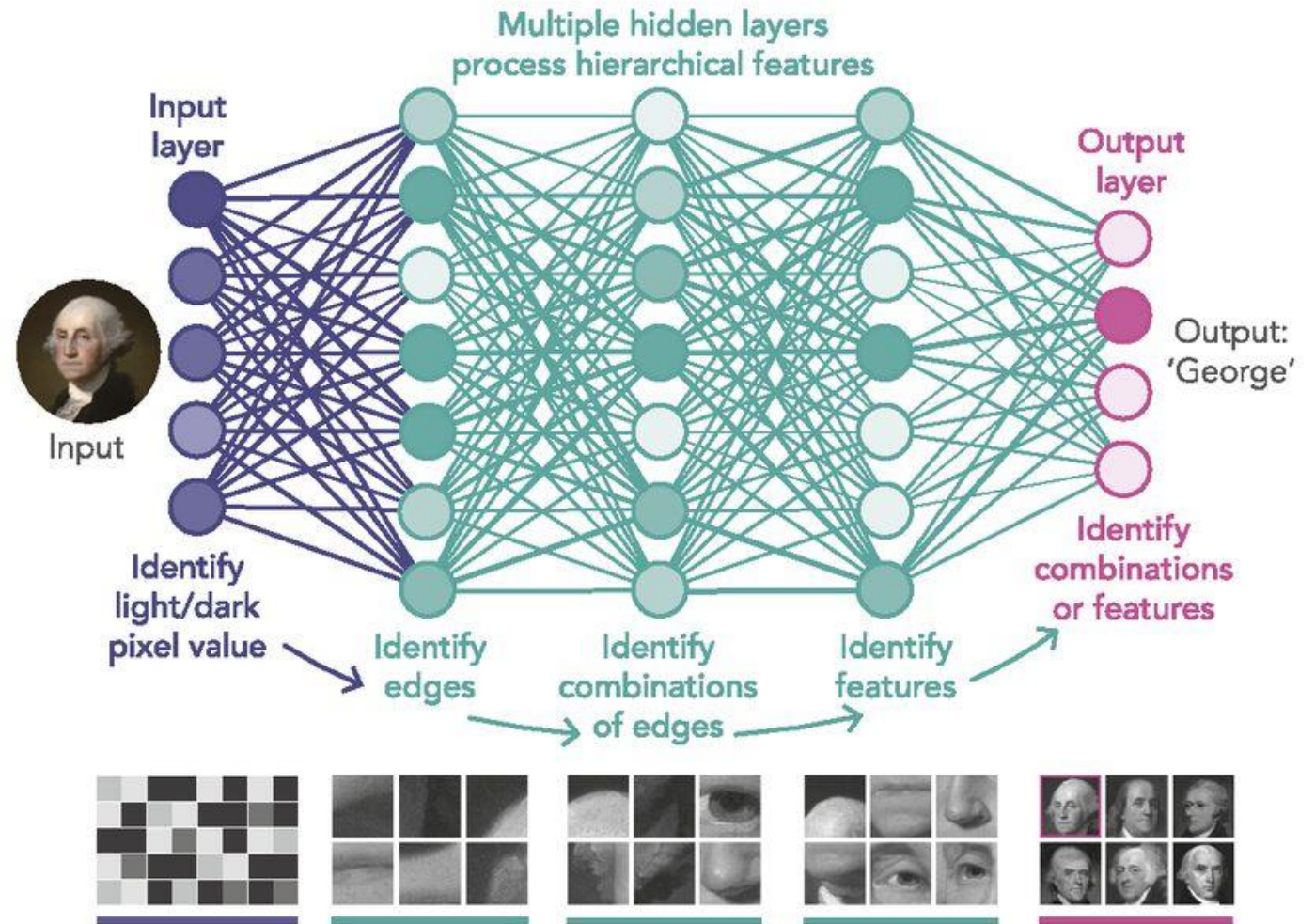
Deep Learning

1980S-ERA NEURAL NETWORK



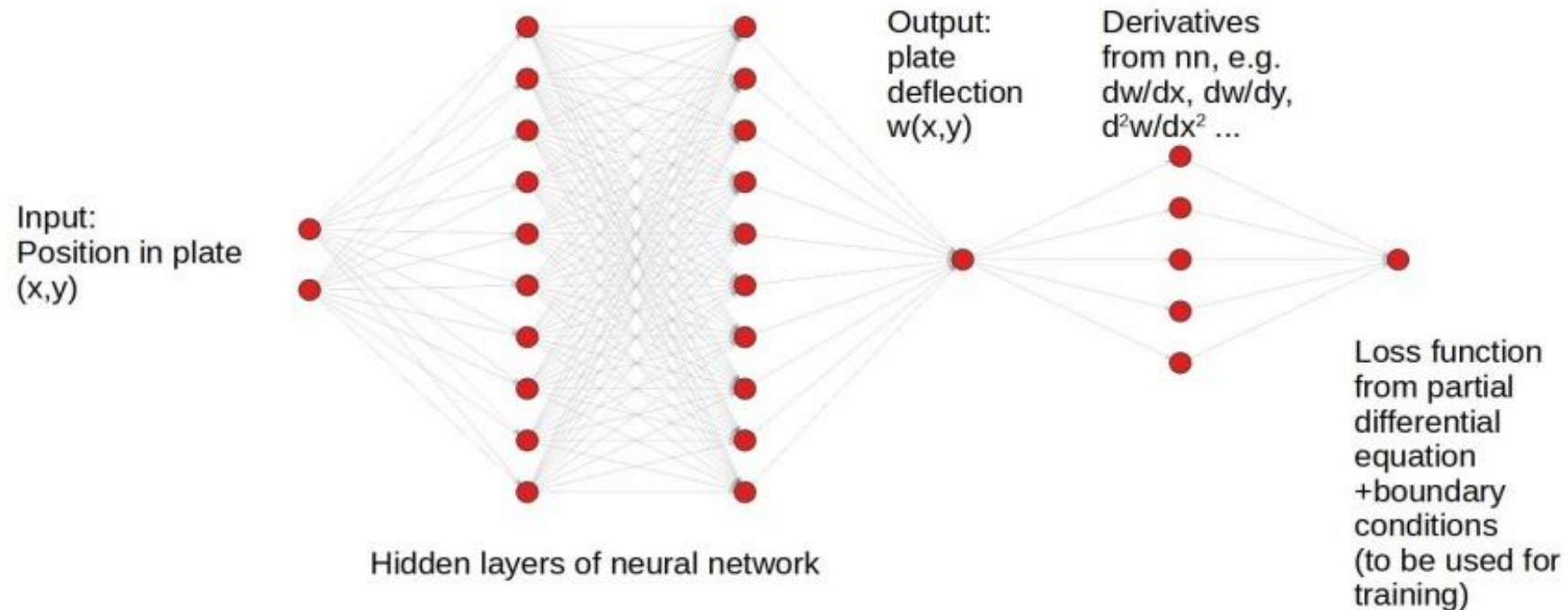
Links carry signals from one node to another, boosting or damping them according to each link's 'weight'.

DEEP LEARNING NEURAL NETWORK

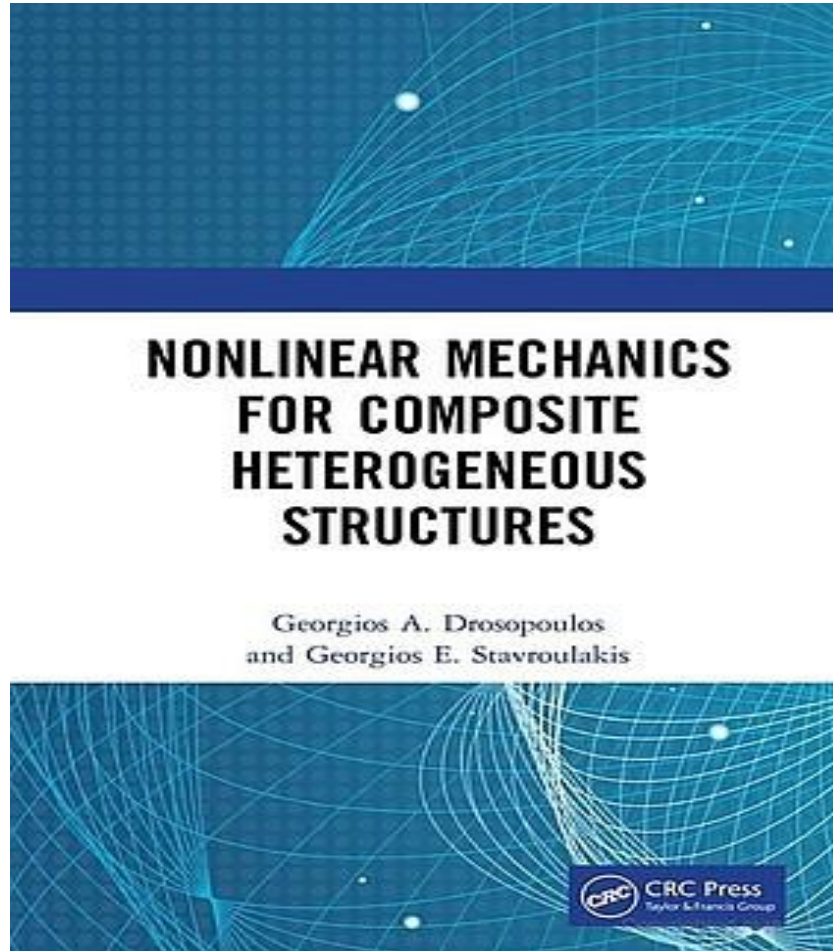


Neural network architecture

The artificial neural network architecture, used in this work is illustrated below.



Our recent book



MATLAB codes for 2-D examples
(homogenization, neural network
integration, XFEM, data-driven)

PYTHON version in preparation

▶ Thank you very much for your attention!

Computational Mechanics and Optimization Laboratory

Email: gestavroulakis@tuc.gr

Web: <http://www.comeco.gr>



For more information you can visit the website



ΠΟΛΥΤΕΧΝΕΙΟ ΚΡΗΤΗΣ
TECHNICAL UNIVERSITY OF CRETE

